Surface-induced ordering and disordering in face-centered-cubic alloys: A Monte Carlo study

W. Schweika
Institut für Festköperforschung, Forschungszentrum Jülich, D-52425 Jülich, Germany

D. P. Landau
Center for Simulational Physics, The University of Georgia, Athens, Georgia 30602;
Institut für Physik, Johannes Gutenberg-Universität Mainz, Staudinger Weg 7, D-55099 Mainz, Germany;
and Höchstleistungsrechenzentrum c/o Forschungszentrum Jülich, D-52425 Jülich, Germany

K. Binder
Institut für Physik, Johannes Gutenberg-Universität Mainz, Staudinger Weg 7, D-55099 Mainz, Germany
(Received 19 September 1995)

Using extensive Monte Carlo simulations we have studied phase transitions in a fcc model with antiferromagnetic nearest-neighbor couplings J in the presence of different free surfaces which lead either to surface-induced order or to surface-induced disorder. Our model is a prototype for CuAu-type ordering alloys and shows a strong first-order bulk transition at a temperature $kT_{cb}/|J| = 1.738\,005(50)$. For free (100) surfaces, we find a continuous surface transition at a temperature $T_{cs} > T_{cb}$ exhibiting critical exponents of the two-dimensional Ising model. Surface-induced ordering occurs as the temperature approaches T_{cb} and the surface excess order and surface excess energy diverges logarithmically. For a free (111) surface, the surface order vanishes continuously at T_{cb} accompanied by surface-induced disorder (SID). In addition to a logarithmic divergence of the excess quantities of order and energy, we find further critical exponents which confirm the actual theory of SID and critical wetting and which can be understood in terms of rough interfaces. For both cases of free surfaces, the asymptotic behavior of the squared interfacial width shows the expected logarithmic divergence.

I. INTRODUCTION

Phase transitions in real crystals are affected by the presence of the surfaces as well as by possible interfaces between ordered domains called antiphase boundaries (APB's). A number of excellent theoretical studies[1–7] have led to detailed predictions for the properties of semi-infinite systems and have been accompanied by some remarkable experimental work in recent years. A review of the related experimental investigations has been given by Dosch.[8] There are different scenarios for how the phase transitions at the surface and in the near-surface region depend on the order of the bulk phase transition.

For second-order bulk transitions we now have a rather good picture of the range of possible surface behavior.[1,2] In some situations the surface undergoes a transition at the bulk transition temperature, but the surface critical behavior is described by critical exponents which differ from both the two-dimensional (2D) as well as bulk 3D values. In other cases, when the exchange in the surface layer exceeds that within the bulk by a sufficient amount, the surface may order above the bulk transition, exhibiting 2D exponents.

The situation in which the bulk undergoes a first-order transition has been considered by Lipowsky[7,9–12] who showed that surface-induced disorder (SID) and surface-induced order (SIO) may then be associated with the bulk transition. One of the most notable results is the continuous decrease of the order parameter in the surface layer as the bulk transition temperature is approached. Such a behavior had already been found in 1973 by Sundaram *et al.* in a low-electron electron-diffraction (LEED) study of a free (100) surface of a Cu_3Au alloy,[13,15] and the critical surface exponent β_1 was later determined by spin-polarized LEED.[16] Monte Carlo (MC) simulations[14] of an Ising model of this alloy also indicated a possible continuous decrease of the surface order as the bulk transition was approached.

From experiments on the same alloy using evanescent x-ray scattering in grazing incidence evidence was found for the increasing thickness of the disordered surface layer as the transition temperature is approached.[17] The related phenomenon of surface melting was observed in lead by ion scattering[18] and confirmed by LEED.[19] In the case of SID there is no clear quantitative experimental evidence up to now for the predicted logarithmic divergence of the thickness of a wetting layer of the disordered phase at the surface. However, such behavior has been observed by transmission electron microscopy for the analogous situation in the bulk of a Cu-Pd (17%) alloy where the width of the antiphase boundaries diverges (logarithmically) as the transition temperature is approached from below.[20] Although discontinuous order-disorder transitions are quite common in alloy systems, most experimental examples consider simple structures showing transitions from a cubic ordered ($L1_2$ in the examples above) to a cubic disordered phase thus avoiding the complications due to the possible strain between ordered variants of lower symmetry. However, as has been shown in a previous Monte Carlo study, the fcc alloys having a Cu-Au-type order ($L1_0$) and tetragonal symmetry are not only candidates for the observervation of SID but also for SIO which may occur because a free (100) surface reduces the

frustration effects.[21] It is the aim of the present work to contribute to the understanding of both SID and SIO by Monte Carlo simulation of a suitable model.

In this paper we consider a simple model for an AB binary alloy which can, of course, be reinterpreted as an Ising magnet, or as a lattice-gas model for a fluid or alloy (spins $S_i = \pm 1$ at lattice site i corresponding to the site being occupied or empty, or containing an A atom or B atom, respectively). For our Monte Carlo simulation, a thick-film geometry is used in which there are two parallel free surfaces, and the nature of the phase transitions in these surfaces forms the subject of this study. By ''thick film'' we mean that the two surfaces can be considered as essentially noninteracting and that our study is meant to address the behavior of semi-infinite bulk systems with free surfaces. Preliminary results have been presented[21] for the case where both nearest-neighbor and next-nearest-neighbor coupling are present, but only a single orientation of the surface (100) was considered [Fig. 1(a)]. We now present results with only nearest-neighbor coupling and two different orientations of free surfaces.

In the following section we describe the theoretical background on SID, to provide the framework in which our study can be interpreted, and motivate the choice of quantities that will be studied. In Sec. III we describe the model and methods used, and in Secs. IV and V we present results for (100) and (111) surfaces [Fig. 1(b)], respectively. We conclude in Sec. VI, while the ground-state behavior and the precise estimation of the bulk transition temperature are discussed in the appendixes.

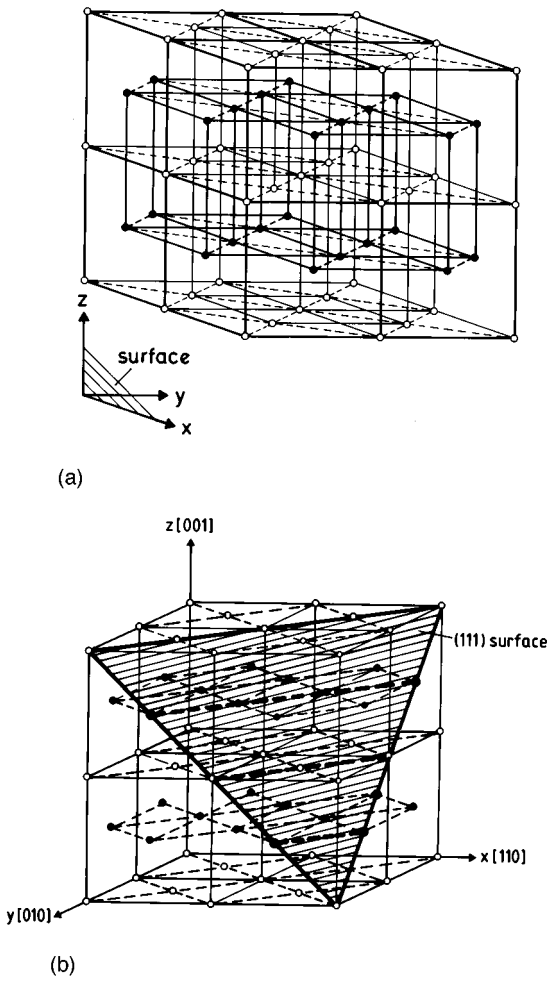

FIG. 1. Section of the ordered lattice of the AB alloy in the $L1_0$ (CuAuI) structure. Frustrated nearest-neighbor interactions are shown by dashed lines. (a) (100) surface oriented such that there is (2×2) order in the surface layer; (b) (111) surface (shaded). Note that in this case a (2×1) order in the surface results, where one-third of the bonds in the surface layer are still frustrated (thick broken lines). Unfrustrated nearest-neighbor interactions are not drawn in order to avoid overcrowding of these pictures.

II. THEORETICAL BACKGROUND

A. Surface-induced disordering

In this section, we recall the basic theoretical predictions on surface-induced disordering (SID) considering only the standard situation which is equivalent to critical wetting[3,7,22] and disregarding other situations which correspond to surface multicritical points.[7,9–12]

The basic phenomenon of interest is the continuous decay of the local order parameter ψ_1 at the surface layer as the first-order transition in the bulk (located at T_{cb}) is approached from below,[9] involving a power law with an exponent β_1

$$\psi_1 \propto t^{\beta_1}, \quad t \equiv (1 - T/T_{cb}) \to 0. \tag{1}$$

This continuous behavior at a discontinuous bulk transition occurs because a layer of the disordered phase gradually intrudes at the surface. For the three-dimensional systems governed by short-range forces it has been predicted that the thickness $\bar{l}$ of this layer (ξ_d being the correlation length of order-parameter fluctuations in the disordered bulk phase) should diverge as

$$\bar{l} \propto \xi_d \ln(1/t), \quad t \to 0, \tag{2a}$$

where one may define a critical exponent

$$\bar{l} \propto \xi_d t^{-\beta_s}, \quad \beta_s = 0(\ln), \quad t \to 0. \tag{2b}$$

Since $\beta_s = 0$ in $d = 3$ dimensions, the divergence of $\bar{l}$ as $t \to 0$ is only logarithmic.[3,7,9–12] As a result, the disordered layer increasingly ''screens'' the effective field acting on the surface layer due to the still well-ordered bulk, and thus Eq. (1) becomes plausible. The interfacial thickness or roughness is expected to diverge as well but more slowly as follows from[22]

$$\xi_\perp / \xi_d \propto [\ln(1/t)]^{1/2}, \quad t \to 0,$$
$$\propto t^{-\nu_\perp}, \quad \nu_\perp = 0(\sqrt{\ln}). \tag{3}$$

As for more standard critical phenomena, one can define a number of divergent response functions to ''fields'' H (conjugate to the order parameter in the bulk) and H_1 (conjugate to ψ_1). Note, that in this case H and H_1 are staggered fields. In the theory of surface effects on bulk critical phenomena[1,2] one distinguishes between the susceptibilities

$$\chi_{1,1}=\left(\frac{\partial\psi_1}{\partial H_1}\right)_t \propto t^{-\gamma_{1,1}}, \quad t\to 0, \tag{4a}$$

$$\chi_1=\left(\frac{\partial\psi_1}{\partial H}\right)_t \propto t^{-\gamma_1}, \quad t\to 0, \tag{4b}$$

and

$$\chi_s=\left(\frac{\partial\psi_s}{\partial H}\right)_t \propto t^{-\gamma_s}, \quad t\to 0. \tag{4c}$$

In Eq. (4c) we have used the surface excess order ψ_s which in turn is defined as the derivative of the surface excess free energy

$$\psi_s=-[\partial F_s(T,H,H_1)/\partial H]_{T,H_1}, \tag{5a}$$

while ψ_1 can be obtained as a derivative with respect to the local field H_1,

$$\psi_1=-[\partial F_s(T,H,H_1)/\partial H_1]_{T,H}. \tag{5b}$$

Finally we mention that the correlation function for order-parameter fluctuations in the surface layer can be used to define a correlation length $\xi_\parallel$,

$$\langle\psi_1(0)\psi_1(\vec{\rho})\rangle-\langle\psi_1\rangle^2\propto\exp(-\rho/\xi_\parallel), \quad \rho\to\infty, \tag{6}$$

where $\vec{\rho}$ is a coordinate in the surface layer, and

$$\xi_\parallel\propto\xi_d t^{-\nu_\parallel}, \quad t\to 0. \tag{7}$$

In order to discuss the scaling relations between these critical exponents for SID, and the theoretical predictions existing for them, we recall that SID can be interpreted as a critical wetting phenomenon.[3,7,22] The scaling relations for critical wetting with short-range forces follow from a scaling analysis for F_s and for $\xi_\parallel$, in terms of scaling functions $\tilde{F}$ and $\tilde{X}$. We use here a superscript "w" in order to avoid confusion between the exponents for critical wetting and the exponents for SID:

$$F_s=\tau^{2-\alpha_s^w}\tilde{F}(\mu\tau^{-\Delta^w}), \tag{8a}$$

$$\xi_\parallel=\tau^{-\nu^w}\tilde{X}(\mu\tau^{-\Delta^w}), \tag{8b}$$

where τ and μ are temperaturelike and fieldlike variables for the wetting transition, α_s^w, ν^w and Δ^w are the associated critical exponents. For $d\leqslant d^*=3$, the upper critical dimensionality for wetting transitions, one has the standard hyperscaling relation

$$2-\alpha_s^w=(d-1)\nu^w \tag{9}$$

for surface excess quantities. Now one can show[3] that for critical wetting there is in fact a *single* independent exponent, since Δ^w also can be related to ν^w

$$\Delta^w=(d+1)\nu^w/2. \tag{10}$$

In $d=3$ dimensions the resulting equations for F_s and $\xi_\parallel$ can hence be written as follows:

$$F_s=\tau^{2\nu^w}\tilde{F}(\mu\tau^{-2\nu^w})=\mu\tilde{f}(\mu^{-1/2\nu^w}\tau) \tag{11a}$$

$$\xi_\parallel=\tau^{-\nu^w}\tilde{X}(\mu\tau^{-2\nu^w})=(\mu)^{-1/2}\tilde{\xi}(\mu^{-1/2\nu^w}\tau). \tag{11b}$$

In the last step we have redefined the scaling functions to express the singularities in terms of μ instead of τ.

Now a comparison of the free-energy functionals of SID and critical wetting shows[3,7,22] that these problems are equivalent to each other if one approaches wetting criticality along a special path (where $\mu\propto\tau$) in the (μ,τ) plane. Since it turns out that the singularities along these paths are the same as along the path ($\tau=0,\mu$ variable), we consider for simplicity singularities along the latter path.

From Eqs. (8a)–(11b) it is easy to derive the critical behavior of the various response functions for this wetting problem. We recall that for critical wetting temperaturelike variables and H_1 scale in the same way, since one can cross the wetting transition line $H_1=H_{1c}(T)$ either by variation of T or of H_1. Therefore, taking a derivative of Eq. (8a) with respect to τ we get

$$\psi_1\propto\tau^{1-\alpha_s^w}\tilde{\psi}_1(\tau\mu^{-1/\Delta^w})_{\tau=0}\propto(\mu)^{(1-\alpha_s^w)/\Delta^w}, \tag{12}$$

where we have indicated how the power law for ψ_1 as function of μ can be inferred by requiring that the corresponding scaling function $\tilde{\psi}_1$ behaves as a power law for small arguments such that the dependence on τ cancels. From Eq. (12) we can read off the value of the exponent β_1

$$\beta_1=(1-\alpha_s^w)/\Delta^w=\frac{2(d-1)-2/\nu^w}{(d+1)}. \tag{13}$$

Using Eqs. (5a) and (8a) we obtain the critical behavior of the excess quantities, in particular of ψ_s:

$$\psi_s\propto\mu^{(2-\alpha_s^w-\Delta^w)/\Delta^w} \tag{14}$$

determining the critical exponent β_s

$$\beta_s=(2-\alpha_s^w-\Delta^w)/\Delta^w=(d-3)/(d+1). \tag{15}$$

Because of the vanishing β_s in $d=3$ one expects a logarithmic divergence of the surface excess order parameter ψ_s, as well as of other excess quantities like the surface excess energy E_s and the thickness of the wetting layer $\bar{l}$ [Eq. (2b)].

Similarly one obtains the surface excess susceptibility, the layer susceptibilities and their exponents, respectively,

$$\chi_s\propto\mu^{-[2-(2-\alpha_s^w)/\Delta^w]},$$

$$\gamma_s=2-\frac{2-\alpha_s^w}{\Delta^w}=\frac{4}{d+1}, (=1 \text{ in } d=3) \tag{16a}$$

$$\chi_1\propto\mu^{-1+(1-\alpha_s^w)/\Delta^w},$$

$$\gamma_1=1-\frac{1-\alpha_s^w}{\Delta^w}=\frac{3-d+2/\nu^w}{d+1}, \tag{16b}$$

$$\chi_{1,1}\propto\mu^{-\alpha_s^w/\Delta^w},$$

$$\gamma_{1,1}=\alpha_s^w/\Delta^w=\frac{-2(d-1)+4/\nu^w}{d+1}. \tag{16c}$$

From Eqs. (13)–(16) one can read off the scaling laws

$$\beta_1+\gamma_1=1, \tag{17a}$$

$$\beta_s+\gamma_s=1, \tag{17b}$$

$$\gamma_{1,1}+\gamma_s=\frac{-2d+6+4/\nu^w}{d+1}=2\gamma_1, \tag{17c}$$

$$\gamma_{1,1}+2\beta_1=\frac{2(d-1)}{d+1}(=1 \text{ in } d=3). \tag{17d}$$

Some of the above relations can be obtained very directly, of course, if we simply replace μ by the temperature distance t and τ by H_1 in Eqs. (11a) and (11b), to find

$$F_s=t\tilde{f}(t^{-1/2\nu^w}H_1), \tag{18a}$$

$$\xi_\parallel=t^{-1/2}\tilde{\xi}(t^{-1/2\nu^w}H_1), \tag{18b}$$

(remember that we have restricted ourselves to $d=3$ here). From Eqs. (8b), (18b) one sees that the exponent $\nu_\parallel$ defined in Eq. (7) for SID is

$$\nu_\parallel=\nu^w/\Delta^w=2/(d+1)(=1/2 \text{ in } d=3). \tag{19}$$

From Eq. (18a) we can immediately recognize the scaling structure of ψ_1 by taking a derivative with respect to H_1,

$$\psi_1=\tau^{\beta_1}\tilde{\psi}_1(t^{-1/2\nu^w}H_1),$$

$$\beta_1=1-1/2\nu^w, \quad d=3, \tag{20}$$

and a further derivative yields $\chi_{1,1}$, the singular part of which scales as

$$\chi_{1,1}=t^{-\gamma_1}\tilde{\chi}_{1,1}(t^{-1/2\nu^w}H_1),$$

$$\gamma_{1,1}=-1+1/\nu^w, \quad d=3. \tag{21}$$

These results contain the mean-field theory of SID,[7,9–12] as a special case: for the mean-field theory of wetting $\nu^w=1$, and hence (in $d=3$)

$$\beta_1=1/2, \quad \gamma_1=1/2, \quad \gamma_{1,1}=0, \quad \Delta^w=2, \quad \alpha_s^w=0, \tag{22a}$$

while the following critical exponents are (independent of ν^w) universal and exact in $d=3$:

$$\beta_s=0, \quad \gamma_s=1, \quad \nu_\perp=0, \quad \nu_\parallel=1/2, \quad \alpha_s=1. \tag{22b}$$

Note that Eq. (18a) can also be interpreted as $F_s=t^{2-\alpha_s}\tilde{f}(t^{-\Delta_1}H_1)$, where the exponents α_s and Δ_1 have the standard meaning as in the usual theory of surface critical phenomena, see Ref. 1, and $2-\alpha_s=(d-1)\nu_\parallel$ is satisfied with $\alpha_s=1$, $\nu_\parallel=1/2$ in $d=3$. We also have $2-\alpha_s=\beta_1+\Delta_1$ and $2-\alpha_s=(2-\alpha_s^w)/\Delta^w$, of course, and $\gamma_s=2\nu_\parallel$. Since $d=3$ is the upper critical dimension for critical wetting, all scaling laws Eqs. (17a)–(17d) are indeed satisfied with these Landau theory exponents, Eq. (22).

Now one knows that fluctuation corrections for critical wetting are possibly very important, and the renormalization-group theories[22–27] predict that ν^w depends on a nonuniversal parameter ω,

$$\omega=k_BT_{cb}/(4\pi\tilde{\Sigma}\, l^2), \tag{23}$$

where T_{cb} is the transition temperature of the bulk, $\tilde{\Sigma}$ is the interfacial stiffness of the interface between the ordered and disordered phase coexisting at T_{cb}, and l is its intrinsic thickness (Lipowsky[7] identifies $l=\xi_d$). The exponent β_1 is predicted to be

$$\beta_1=1/2+\omega/2, \quad 0<\omega\leqslant 1/2, \tag{24a}$$

$$\beta_1=\sqrt{2\omega}-\omega/2, \quad 1/2<\omega\leqslant 2, \tag{24b}$$

$$\beta_1=1, \quad \omega\geqslant 2. \tag{24c}$$

[Note that because of Eq. (20) this prediction is simply equivalent to those of Refs. 22–27 for the exponent ν^w discussed in the theory of critical wetting.] Results for other exponents simply follow from the scaling relations written down above. It is, however, of interest to show the relation for the logarithmic relations for the thickness of the surface near layer $\bar{l}$ and the width $\xi_\perp$ of the (rough) interface[7,22]

$$\bar{l}/\xi_d=1/2[1+2\omega]\ln(1/t), \quad 0<\omega\leqslant 1/2, \tag{25}$$

$$\xi_\perp/\xi_d=\sqrt{\omega}[\ln(1/t)]^{1/2}, \quad 0<\omega\leqslant 1/2. \tag{26}$$

Here we have restricted ourselves to the regime $\omega\leqslant 1/2$, which is of most interest. Note that while a direct determination of ω from Eq. (23) is difficult, since it is hard to calculate $\tilde{\Sigma}$, one could infer its value indirectly if Eqs. (25) and (26) are used. However, in computer simulation studies of wetting in the Ising model[29–31] it was already not possible to verify the predictions[22–27] for ν^w that correspond to Eqs. (24a)–(24c). The interpretation of these findings is uncertain: It has been proposed that one must be extremely close to the transition to see the asymptotic behavior,[26] or that the wetting transition is weakly of first order.[27] (Boulter and Parry have recently proposed another explanation.[28] This will be further discussed later.) It is unclear to us whether these latter predictions should apply to the present problems as well.

It should be stressed that Eqs. (23)–(26) can apply only if the interface between the ordered and disordered phase is rough. Lipowsky[7] supposed that Eq. (22a) is valid if one is below the roughening transition temperature of this interface. In view of Monte Carlo studies and of molecular field calculations for semi-infinite Potts model[33] on wetting near the roughening temperature of the Ising model,[32] we would like to mention the possibility that for nonrough interfaces SID might be replaced by a sequence of layering transitions. An effective exponent $\beta^{\text{eff}}=\frac{1}{2}$ can then be defined only in the sense that the sequence of steps in a log-log plot is approximated by a straight line.[7]

B. Surface-induced ordering

While SID and SIO are commonly discussed in the literature to be just equivalent phenomena, one has to note one important difference, namely that for SIO the surface necessarily orders at a different and higher temperature than the bulk in order to wet the bulk phase. An estimate for the surface transition temperature can be obtained from a comparison to the two-dimensional model. Hence, one expects

$T_{cb}<T_{cs}<T_c^{2D}$. One important consequence is that the predictions for the surface properties, and also the scaling relations discussed above, can no longer be valid. Instead, at the surface transition one expects a behavior which falls in the universality class of the corresponding purely 2D system. The exponent $\nu_\parallel$ describing the singularity of $\xi_\parallel$, $\xi_\parallel \propto (T-T_{cs})^{-\nu_\parallel}$, is simply the bulk 2D exponent $\nu(d=2)$, and the exponent β_1 describing the order parameter $\psi_1 \propto (T-T_{cs})^{-\beta_1}$ is the bulk 2D exponent $\beta(d=2)$. Note that at T_{cs} the susceptibilities χ_{11}, χ_1, and χ_s *all have the same singularity* [$\chi \propto |T-T_{cs}|^{-\gamma(d=2)}, \gamma(d=2)$ being the 2D bulk susceptibility exponent]. The scaling relations for the surface exponents at T_{cs} thus are just standard bulk scaling laws.

For $T \to T_{cb}$ the logarithmic law for the excess quantities, e.g., those of the order, the energy, and the interface position, should still be valid. Surface properties are expected to show an ''extraordinary'' transition[1,2] (singularities in the second derivatives, kink in ψ_1).

III. MODEL AND SIMULATION TECHNIQUE

We study the Ising Hamiltonian on the face-centered-cubic lattice in a $L \times L \times D$ geometry, applying periodic boundary conditions in x and y directions. The two free $L \times L$ surfaces are oriented to be either (100) or (111) faces. The Hamiltonian used is

$$\mathscr{H} = -J \sum_{\langle i,j \rangle} S_i S_j, \quad S_i = \pm 1, \tag{27}$$

where the sum is over all nearest-neighbor pairs (i,j) with antiferromagnetic nearest-neighbor coupling, i.e., $J<0$. Note that in the present case, the atoms in the surface layers do not have any modified nearest-neighbor coupling, but they do, of course, see fewer neighbors than do those atoms in the bulk. We used a Metropolis, single spin-flip method with preferential layer sampling which was determined by the nature of the order-parameter profile. We implemented an efficient, vectorized single spin-flip algorithm on a CRAY-YMP computer. Since our aim was to gain an overview of the system behavior for a wide range of temperatures, excessively large values for L were avoided. Typically L varied from 32 to 128, and thicknesses studied varied from $D=40$ to $D=200$ to ensure that the two surfaces were independent.

In principle, a complete description of the CuAu-type order requires a three-dimensional order parameter $\psi=(\psi_x,\psi_y,\psi_z)$ which refers to the three possible orientations of ordered domains, which are alternate layering of pure Cu and pure Au planes in one of the three $\langle 100 \rangle$ directions. The components of the order parameter are necessarily based on four sublattices and can be defined for bilayers only. For example, the first component $\psi_{x,n}$ the order parameter of the bilayer n is defined as

$$\psi_{x,n} = \frac{1}{L^2} \sum_{j \epsilon \text{ bilayer } n} S_j e^{i\mathbf{k}\cdot\mathbf{r}_j}, \text{ where } \mathbf{k} = \frac{2\pi}{a}(1,0,0). \tag{28}$$

Using the sublattice magnetizations m_1, m_2, m_3, and m_4 one obtains

$$\psi_{x,n} = \frac{1}{4}(m_1 - m_2 - m_3 + m_4)$$

$$\psi_{y,n} = \frac{1}{4}(m_1 - m_2 + m_3 - m_4)$$

$$\psi_{z,n} = \frac{1}{4}(m_1 + m_2 - m_3 - m_4). \tag{29}$$

Similarly, one can define a total order parameter for the whole film and a bulk order parameter for the inner part of the film. However, in most cases, the anisotropy of the systems considered is sufficiently strong to single out only one component of order, while the other two components, as well as their fluctuations, are negligible. This holds throughout for the case of SID at the free (111) surface. In other words, in the ordered phase the symmetry is broken, and only one type of domain is considered (which in the simulation is created by preparation of the initial state). Since the transition is of first order in the bulk, the system does not ''jump over'' to the orderings corresponding to the other types of domains, at least not for the large lattice sizes studied. In these cases, it is justifiable to confine ourselves to a two sublattice order parameter

$$\psi_{y,n} = \frac{1}{2}(m_1 - m_2), \tag{30}$$

which is simply a single layer order parameter and a scalar quantity. Both types of order parameters, and their related susceptibilities, were calculated in the simulations. The surface excess order parameter is obtained by

$$\psi_s = \sum_{n=1}^{D/2} \{\psi_n - \psi_b\}. \tag{31}$$

The (bi-)layer susceptibilities χ_n and $\chi_{n,n}$ were obtained from the fluctuation relations[34]

$$\chi_{n,n} = L^2(\langle \boldsymbol{\psi}_n \cdot \boldsymbol{\psi}_n \rangle - \langle \boldsymbol{\psi}_n \rangle \cdot \langle \boldsymbol{\psi}_n \rangle)/k_B T, \tag{32}$$

$$\chi_n = L^2 D(\langle \boldsymbol{\psi}_n \cdot \boldsymbol{\psi}_{\text{tot}} \rangle - \langle \boldsymbol{\psi}_n \rangle \cdot \langle \boldsymbol{\psi}_{\text{tot}} \rangle)/k_B T, \tag{33}$$

while the surface excess susceptibility χ_s follows as

$$\chi_s = \sum_{n=1}^{D/2} \{\chi_n - \chi_b\}. \tag{34}$$

Here, χ_b denotes the (bi-)layer susceptibility in the bulk. The surface layer susceptibilities χ_1 and the excess susceptibilities χ_s were also calculated according to their definitions as derivatives in Eqs. (4b) and (4c). As discussed in Appendix C, there are no fluctuation relations analogous to Eqs. (32) and (33) for the excess quantities such as χ_s.

Furthermore, we considered the layer energies E_n (normalized per spin), the bulk and total energies E_b and E_{tot}, the surface excess energy E_s, the layer specific heat C_n, and the surface excess specific heat C_s:

$$E_s = \sum_{n}^{D/2} (E_n - E_b), \tag{35}$$

$$C_n = L^2 D(\langle E_n E_{\rm tot}\rangle - \langle E_n\rangle\langle E_{\rm tot}\rangle)/T^2, \tag{36}$$

$$C_s = \sum_n^{D/2} (C_n - C_b). \tag{37}$$

For locating the transition of the first layer in case of SIO, we used the reduced cumulant

$$U_{1,L} = 1 - \langle \psi_1^4\rangle/(3\langle \psi_1^2\rangle^2). \tag{38}$$

In order to fit the layer profiles we used the following formula:

$$\psi_n = \psi_{\rm max}[1 + \exp(-2\xi_\perp^{-1}(n-\hat{n}))]^{-1}, \tag{39}$$

where $\hat{n}$ is the interface position and $\xi_\perp$ the interface width. Note, that the inverse of the gradient of ψ_n equals twice that of $\xi_\perp$. This formula is analogous to the tanh function of the interfacial profile between two ordered domains at a second-order bulk transition.[39]

The typical run length varied from an average of 10^4 Monte Carlo steps/site to an average of 10^5 Monte Carlo steps/site near T_{cb} for the larger choices of L. We speak of an ''average'' number of spin flips because the different layers were not sampled equally. For studies of wetting, layering, and surface critical phenomena,[29–32,34] we have found it useful to consider sites near the free surfaces more often for a spin flip than sites in the bulk (''preferential surface site selection''). Here the situation is different; the surface fields suppress fluctuations in the layers very close to the surfaces, and the largest and slowest fluctuations do *not* occur in the bulk. In many cases considered they also do not occur at the surface but rather at, or near, the interface (which is typically a few layers away from the surface). Therefore, we choose either a ''preferential surface site selection'' which decays exponentially to a constant with n, or one in which the choice is proportional to the gradient $\partial\psi_n/\partial n$. We also carried out multiple, independent runs with different random number sequences to obtain estimates for the statistical errors.

Previous calculations[40–47] of the bulk transition temperature T_{cb} for this model do not have the precision required for the present study. Therefore, the transition temperature of the bulk alloy was determined by standard thermodynamic integration of data for large systems with fully periodic boundary conditions. We estimate that $k_B T_{cb}/|J| = 1.738\,005 \pm 0.000\,050$. A more detailed description of this study is presented in the Appendix A.

IV. RESULTS FOR (100) SURFACES

In Fig. 2(a) we show the temperature variation of the surface layer order parameter ψ_1 and the bulk order parameter ψ_b. This figure clearly shows the large jump in bulk order which occurs at T_{cb}, but it is also obvious from this plot that surface order begins to develop well above the bulk transition. The surface order increases as the temperature is lowered, and it smoothly alters when the bulk finally undergoes a discontinuous transition. At the first-order bulk transition temperature T_{cb} one notices a kink in $\psi_1(T)$, as one may expect for an ''extraordinary transition.'' [In the literature,[1,2,48,49] the extraordinary transition of an ordered surface at a second-order transition is primarily discussed: then $\psi_1(T)$ has no kink, since the singularity of ψ_1 is the same as that of the bulk free energy density, $f_b \propto |1 - T/T_{cb}|^{2-\alpha_b}$: ψ_1 then has a singularity only in its curvature at T_{cb}.[48] At a first-order transition, f_b has a kink singularity, and so does ψ_1.]

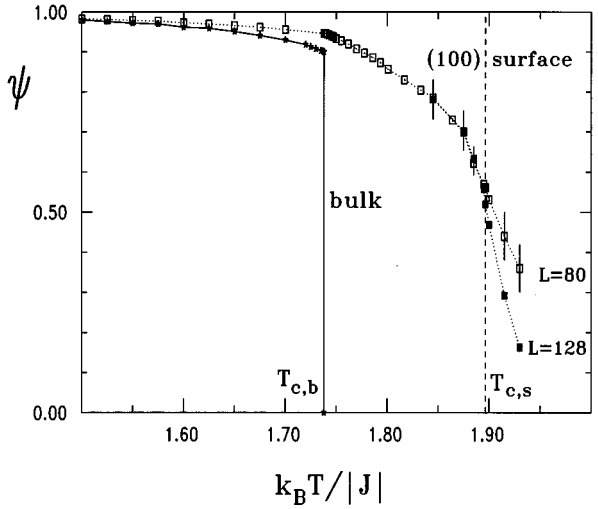

FIG. 2. Temperature dependence of the surface layer order parameter ψ_1 (broken curve) and the bulk order parameter ψ_b (full curve) for the case of our (100) surface. Two linear dimensions ($L = 80$, 128) are included to show the onset of size effects at T_{cs}.

Furthermore there are obvious finite-size effects at the surface ordering transition. The nature of the surface ordering transition and the critical behavior of our model is expected to be same as for a two-dimensional Ising model, since obviously the (2×2) order of the ordered surface plane has this symmetry. Since the surface transition temperature is above the first-order bulk transition temperature T_{cb} the nature of the surface transition is, of course, independent of any wetting properties which occur as $T \to T_{cb}$.

The manner in which the surface order propagates into the bulk as the temperature is lowered can be seen in Fig. 3 where we present some profiles of the order parameter and layer energy for a thick film of size $L\times L$ with $L = 80$ and thickness $80 < D < 200$. These large thicknesses ensure that the two free surfaces are independent of each other, as can be verified very nicely from the pair-correlation function data shown in Fig. 3(c): correlations parallel and perpendicular to the free surfaces are identical in the bulk. At the interface the correlations remain anisotropic and do not obey the symmetry properties of the disordered cubic phase. The perpendicular correlations across the interface determine the wetting process. The related correlation length should remain finite as T approaches the first-order transition at T_{cb}; however, this correlation length is not simply the correlation length of the disordered bulk phase as it is usually assumed in the literature.[7] Furthermore, even in the disordered phase the correlations can be anisotropic, and this must be taken into regard when choosing a ''typical'' bulk correlation length. In particular, this is true for the present model as shown in Fig. 4. The largest correlation length is found for the $\langle 100\rangle$ directions, $\xi_{\langle 100\rangle} \approx 4.3$ in units of $a/2$ at T_{cb}.

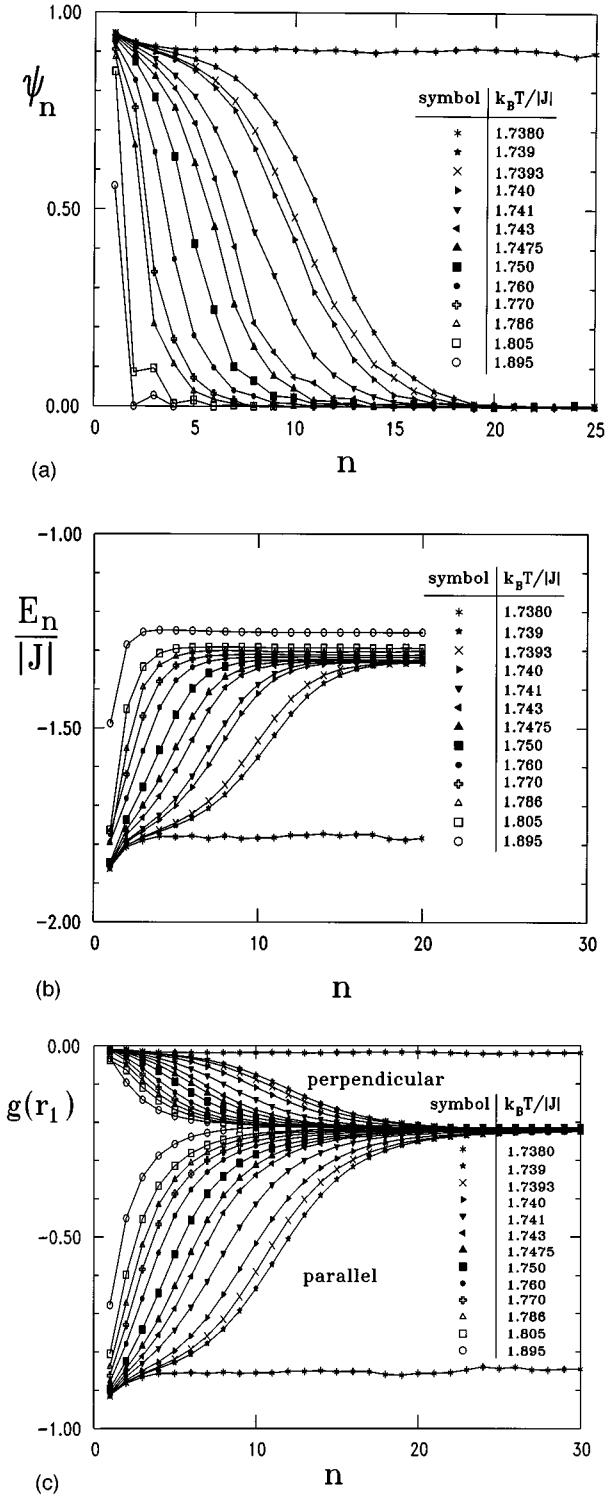

FIG. 3. Profiles for the (100) surface case: (a) the layer order parameter ψ_n; (b) the normalized layer energies $E_n/|J|$ where J is the nearest-neighbor exchange constant; (c) the nearest-neighbor correlation function $g(\vec{r}_1)$ both for $\vec{r}_1$ parallel and perpendicular to the free surface.

The width of the ordered layer grows with decreasing temperature and the profile develops into an S-shaped curve. It can be seen, that the gradient gradually decreases as the interface moves into the bulk with decreasing temperature. While for temperatures slightly below the surface transition

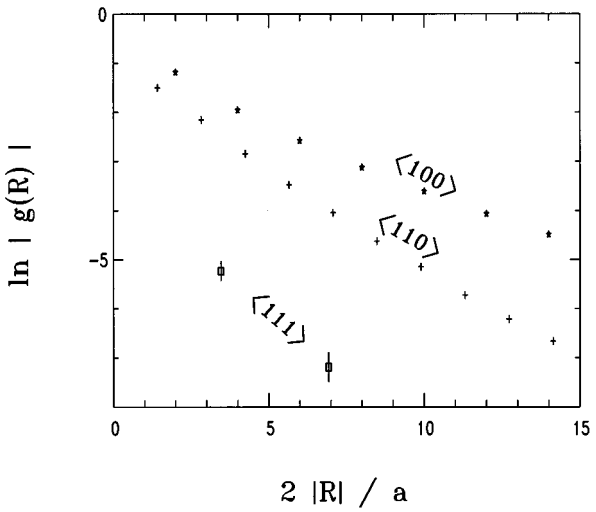

FIG. 4. Anisotropy of the correlations in the disordered (bulk) phase at T_{cb} shown for the three directions $\langle 100\rangle$, $\langle 110\rangle$, and $\langle 111\rangle$ (simulated with full periodic boundary conditions, size: four sc sublattices, each of $L^3=69^3$). The largest correlation length is seen in $\langle 100\rangle$ directions, $\xi_{\langle 100\rangle}\approx 4.3\ a/2$.

T_{cs} the evaluation of the gradient needs a proper analysis of finite-size effects, we found that finite-size effects are not so important for lower T above T_{cb} (at least for the large systems considered). To a good approximation the order-parameter profiles can be fitted to Eq. (39) as shown for example in Fig. 5. Apart from slight deviations close to the surface, this provides an accurate determination of the position $\hat{n}$ and width $\xi_\perp$ of the interfaces. The results for the thickness of the ordered surface layer $\bar{l}$ (which equals $\hat{n}-1/2$) and for the squared width $\xi_\perp^2$ versus the reduced temperature t reveal the theoretically expected asymptotic logarithmic behavior for a rough interface in the limit $T\to T_{cb}$. However, the more detailed predictions given by Eqs. (25) and (26) are in disagreement with the present results. Identifying $\xi_{\langle 100\rangle}$ (as obtained in Fig. 4) with ξ_d yields $\omega=0.16$ which is conceivable in view of the results for the interfacial properties in case of SID at the (111) surface discussed below. However, these values and Eq. (26) would result in a slope $\partial\xi_\perp^2/\partial\ \ln t\approx -3$ which is inconsistent with the data in Fig. 5(c) (slope≈ -5.2). In recent work[28] Boulter and Parry pointed out that the theory of wetting phenomena should not be formulated only in terms of the interfacial position $\bar{l}$, but should include the coupling of $\bar{l}$ to a second length scale l_1; this length scale l_1 describes the range over which the surface causes deviations from the simple interfacial profile, precisely as we see them in Fig. 5(a). It is conceivable that such effects influence the interpretation of some of our results. Of course, one also has to discuss whether the roughening transition T_R for the (100) interface may be above T_{cb}, in which case a qualitatively different behavior results, where the width remains finite and is determined by the finite range of correlations of the homogeneous bulk phases. A crude estimate for T_R may be the transition temperature of the purely 2D system, which is indeed above T_{cb}, and even above T_{cs}. For further comparison, model calculations [MC and cluster variation method (CVM) for the same interaction model][50] show that the width of the

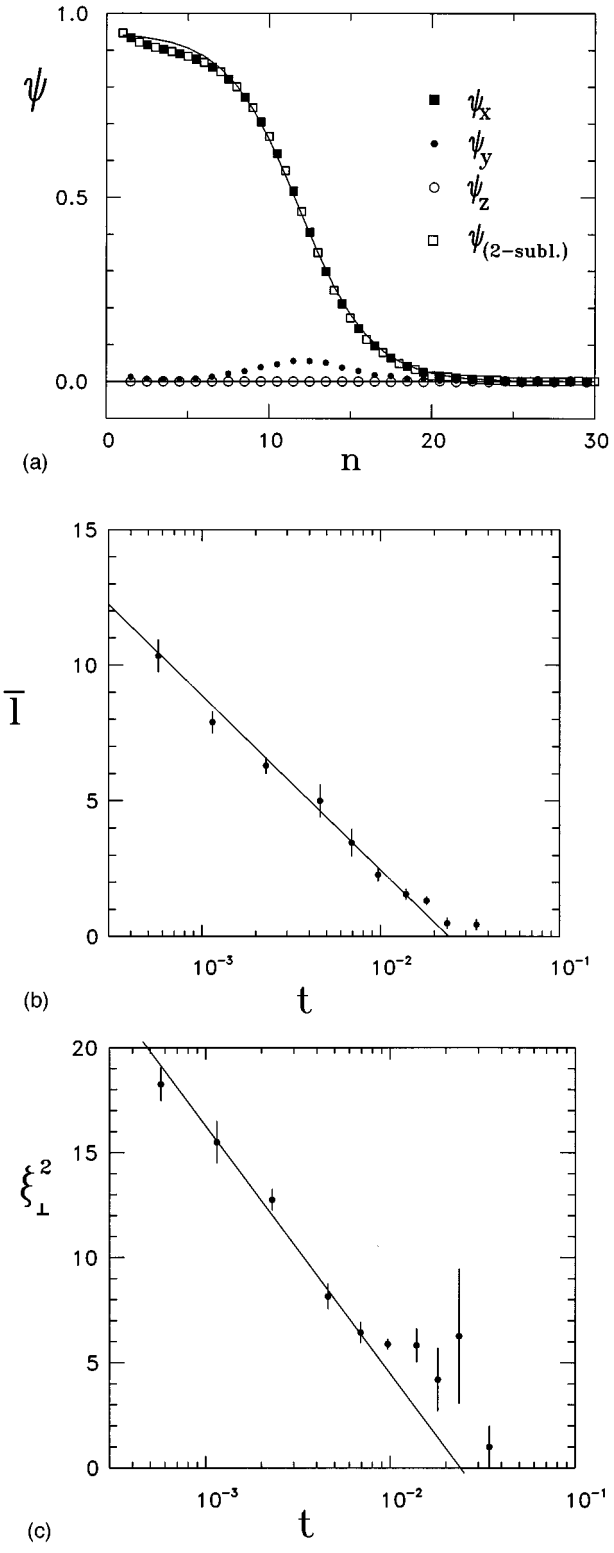

FIG. 5. (a) Fit (dotted line) of the order-parameter profile for a (100) surface using Eq. (39). Data refer to a simulation at $T=1.739|J|/k_B$ for $L\times L\times D=80\times 80\times 180$. (b) Semi-log plot of thickness of the ordered surface layer $\bar{l}$ $(=\hat{n}-1/2)$ vs t; (c) semi-log plot of the squared width of the interface ξ^2 vs t. $\bar{l}$ and ξ^2 have the expected asymptotic behavior, however, the more detailed predictions of Eqs. (25) and (26) are not confirmed.

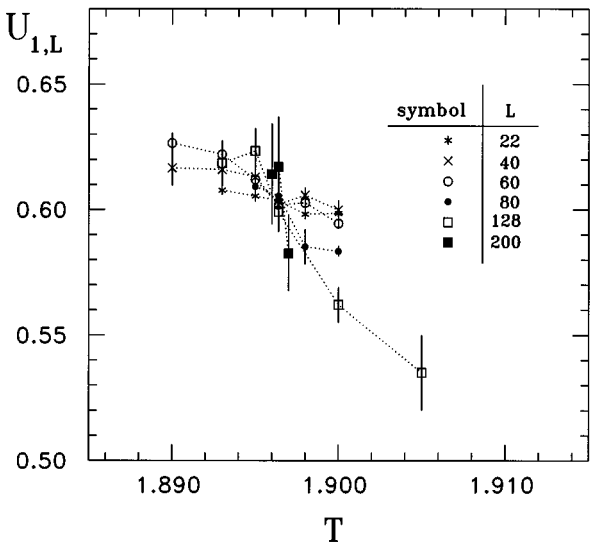

FIG. 6. Variation of the fourth-order cumulant for the surface layer with temperature for different values of L for the (100) case.

(100) interface for the Cu_3Au stoichiometry is large (10 fcc cubes) but finite at T_{cb}. Our data are not sufficient to give a clear and definite answer to this aspect whether the interface eventually becomes rough or not.

While in our preliminary communication[21] on a related model (including a next-nearest-neighbor interaction as well) the behavior of the profiles of order parameter and energy was qualitatively very similar to the data shown in Fig. 3, the statistical accuracy of these old data simply was not good enough to locate the surface transition temperature T_{cs} with sufficient precision to make any meaningful statement about the critical behavior of that model. Thus, in the present work, we take up this problem again: Fig. 6 shows that our present data (which span a range of linear dimensions from $L=32$ to $L=200$) can locate T_{cs} with reasonable precision, namely

$$kT_{cs}/J=1.896\pm 0.001. \tag{40}$$

The cumulant intersections (see Refs. 35–37 for the finite-size scaling background that justifies this method) also are compatible with a value $U_1^*=0.61\pm 0.01$, i.e., within our accuracy this number is compatible with the value for the two-dimensional Ising universality class.[38] This conclusion is supported by a finite-size scaling[33–37] analysis: Fig. 7(a) shows that the variation of the order parameter at T_{cs} is compatible with $\beta/\nu=1/8$, as expected; furthermore, the opposite curvature for temperatures $T>T_{cs}$ and $T<T_{cs}$ supports our belief that our estimate of T_{cs} is correct. From the slope of the cumulants at T_{cs} [see Fig. 7(b)] we extract an exponent $\nu=0.9\pm 0.1$ which is consistent with the 2D Ising value. Of course, the accuracy of our exponent estimates still clearly is not yet very impressive, but since the data in Figs. 6 and 7 have already required a large CPU effort, it will not be easy to improve these estimates further.

The second layer remains disordered at T_{cs} which justifies the choice of the scalar two sublattice layer order parameter for the consideration of the surface transition and explains why the exponents we found agree with those of the 2D Ising universality class. Using the same method of analyzing the

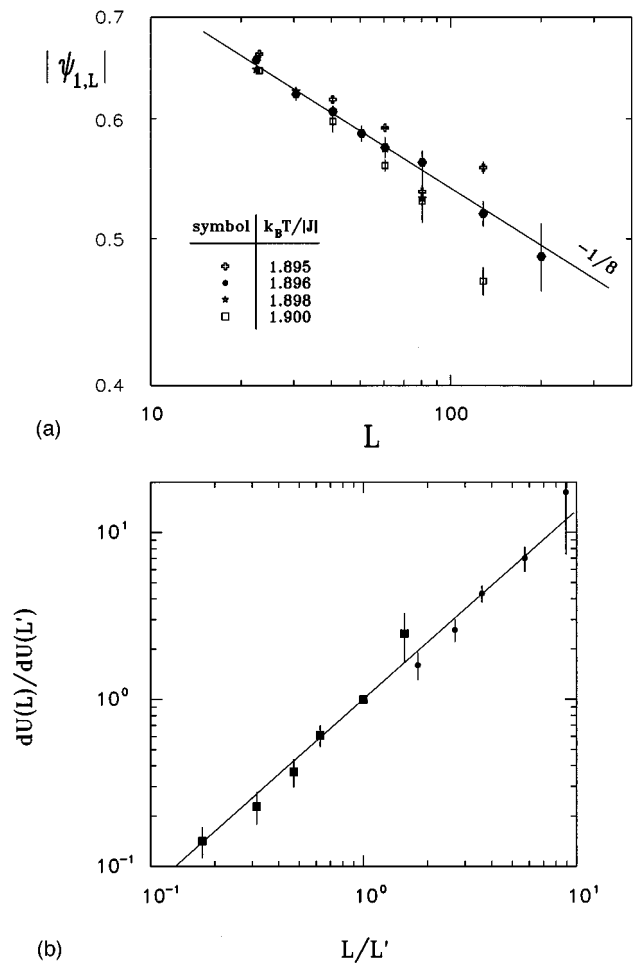

FIG. 7. (a) Log-log plot of the (100) surface order parameter ψ_1 vs L where four different temperatures close to T_{cs} are included; straight line shown has been drawn with the theoretical slope of $-1/8$. (b) log-log plot of the derivative of the cumulant versus the ratio of sizes L/L' (squares: $L'=128$, dots: $L'=22$). Straight line shown has a slope of $1/\nu$ with $\nu=0.9$.

finite-size effects we again found, within the accuracy of our simulations, a continuous ordering transition of the second layer at $kT_{c,n=2}/J=1.791\pm0.003$, with exponents β and ν which are still compatible with those of the 2D Ising model.

However, the wetting phase does not further proceed via a sequence of continuous layer transitions, since as mentioned above the gradient at the interface becomes finite and decreases as T approaches T_{cb}. More precisely, we found that the transition in the first layer is accompanied by the transition in the third layer (and further odd layers), although the amplitude is much smaller. With the ordering of the second layer there is an analogous transition in the subsequent even layers again with exponentially decaying amplitudes. This picture appears to be at least plausible, since the competing $L1_0$ ordering variants ψ_x and ψ_y of the full four sublattice order parameter lead the same scalar order parameter ψ_n for odd layers n, but to ψ_n which are different in sign for even layers n. Furthermore, the additional degeneracy of the ground state, which could lead to APB's and would disturb this type of ordering, is already lifted at finite temperatures (as it is for the infinite system).

Finally, we consider the surface induced ordering in more

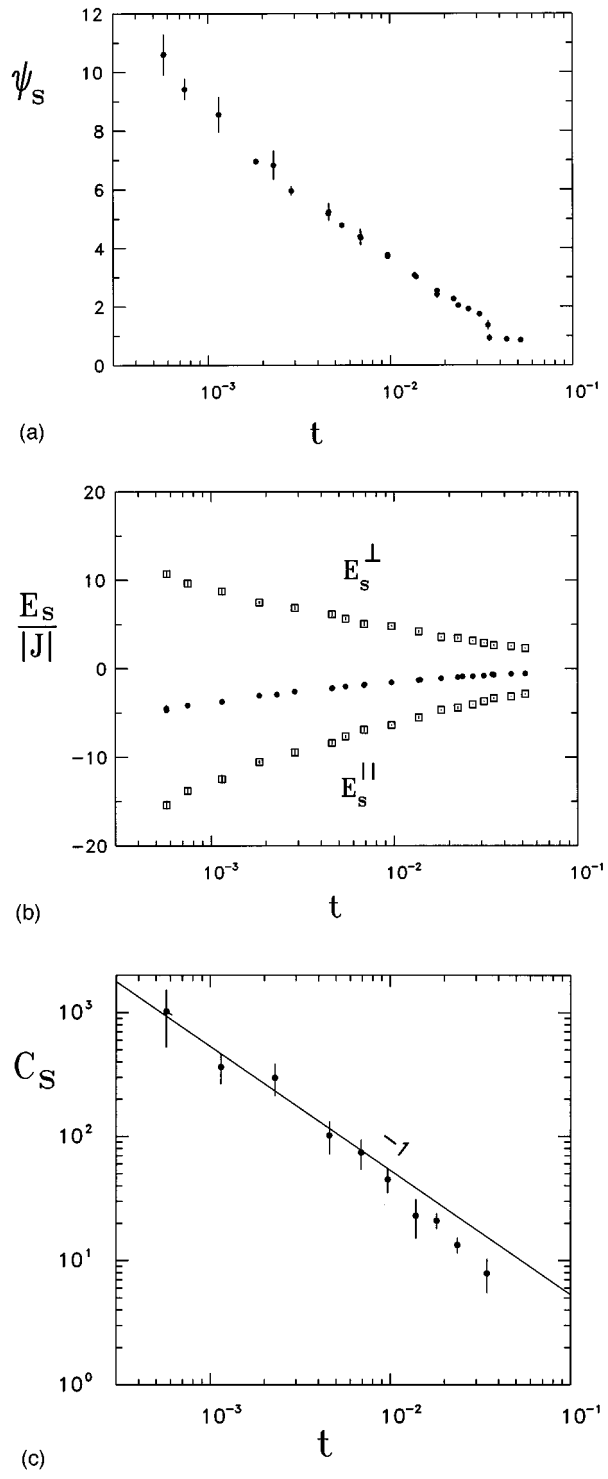

FIG. 8. Semi-log plot of (a) the surface excess order ψ_s vs t and of (b) the surface excess energy E_s vs t (total, parallel, and perpendicular parts); log-log plot of (c) the surface excess specific heat C_s for the (100) case. For comparison the slope -1 corresponding to $\alpha_s=1$ is given.

detail. Figure 8 shows that the surface excess quantities are compatible with the behavior expected theoretically[7,9–12] for a SIO transition: ψ_s and E_s are compatible with logarithmic divergences as $t\to0$ $(T\to T_{cb})$. Here, for the case of SIO we define the reduced temperature variable as $t_{(+)}=1-T_{cb}/T$. The excess specific heat was obtained by use of the appro-

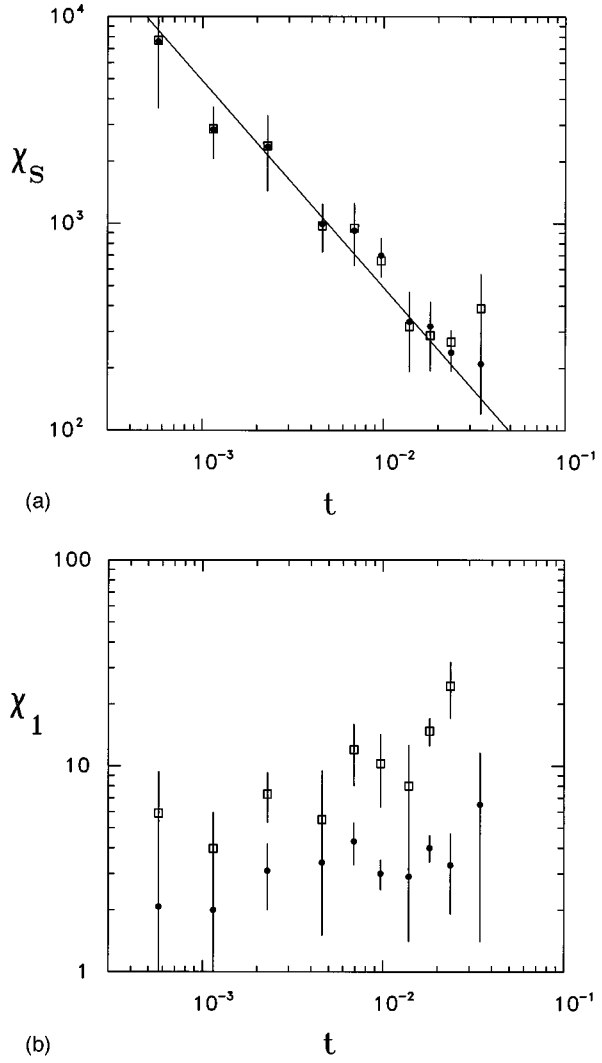

FIG. 9. Log-log plot of (a) the surface excess susceptibility χ_s vs t and of (b) the surface susceptibility χ_1 vs t in case of a (100) surface. Full dots (open squares) represent data based on the scalar two sublattice order parameter (the 3D four sublattice order parameter). χ_s slowly enter the asymptotic region, where the theoretically expected modulus of the slope is given by $\gamma_s=1$.

priate fluctuation relation [see Eqs. (36) and (37)] and is compatible with a Curie-Weiss-like divergence, $C_s \propto t^{-1}$, i.e., $\alpha_s=1$.

In Fig. 9 we analyze the asymptotic behavior of the susceptibilities χ_s and χ_1. The data for χ_s are essentially the same if one considers the fluctuation of a scalar two sublattice layer order parameter or of the full 3D order parameter for bilayers. They are in agreement with the theoretical expectation for the exponent $\gamma_s=1$. The statistical accuracy of the layer susceptibilities χ_1 is not overwhelming. However, both layer and bilayer data seem to approach a constant value in the asymptotic limit $T \to T_{cb}$, which means that $\gamma_1=0$. Any comparison with the theoretical predictions discussed in Sec. II A have to be made with care, since here (and generally for SIO) T_{cs} and T_{cb} do not coincide. Instead, there is only an extraordinary transition at T_{cb} and hence a vanishing exponent γ_1 may be expected.

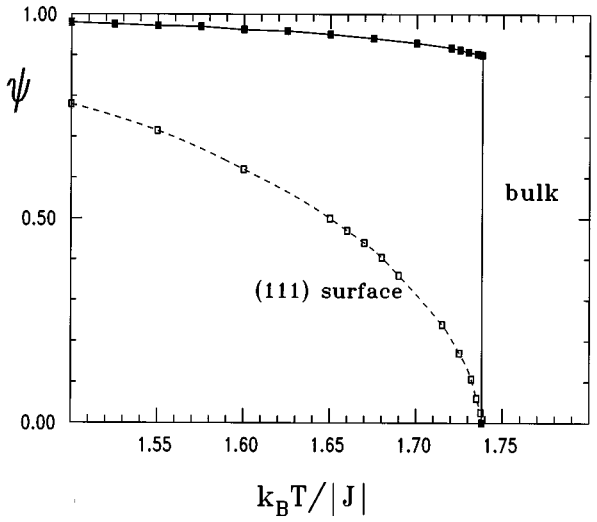

FIG. 10. Temperature dependence of the surface layer order parameter ψ_1 (broken curve) and the bulk order parameter ψ_b (full curve) for the case of an (111) surface.

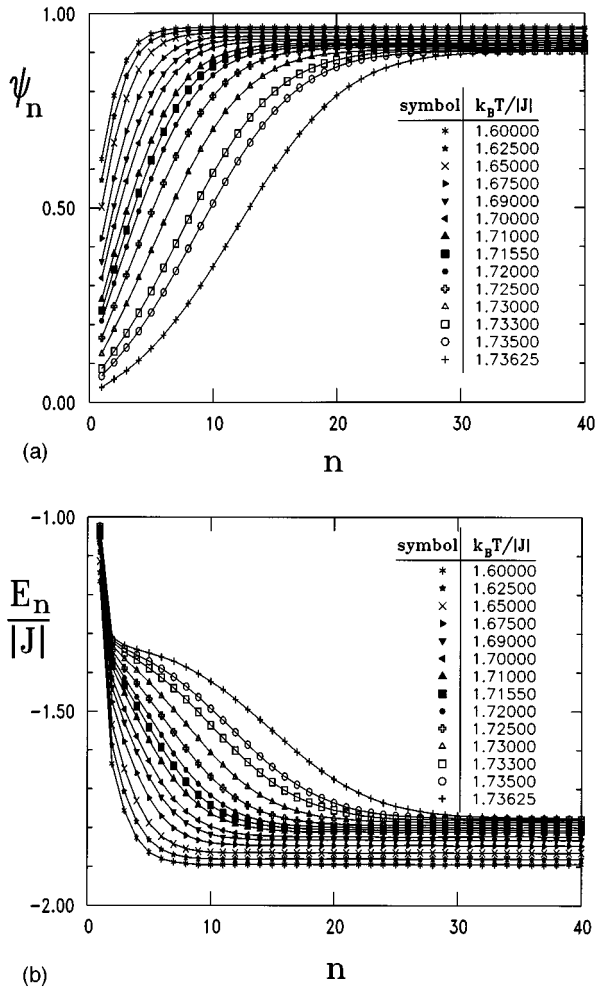

FIG. 11. Profiles for the (111) surface case: (a) layer order parameters ψ_n; (b) normalized layer energies $E_n/|J|$ plotted versus layer number n.

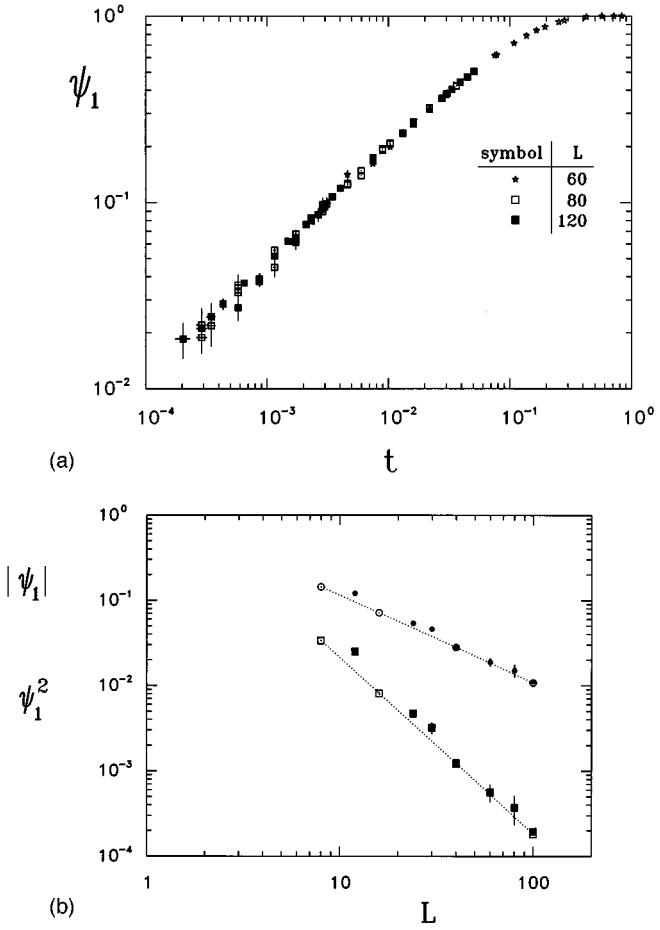

FIG. 12. (a) Log-log plot of the surface layer order parameter for the (111) case vs t; (b) log-log plot of the surface layer order parameter at T_{cb} vs L. Here open or filled symbols refer to runs where the bulk is disordered or ordered, respectively. Straight lines have slopes of about -1.04 and -2.06, respectively.

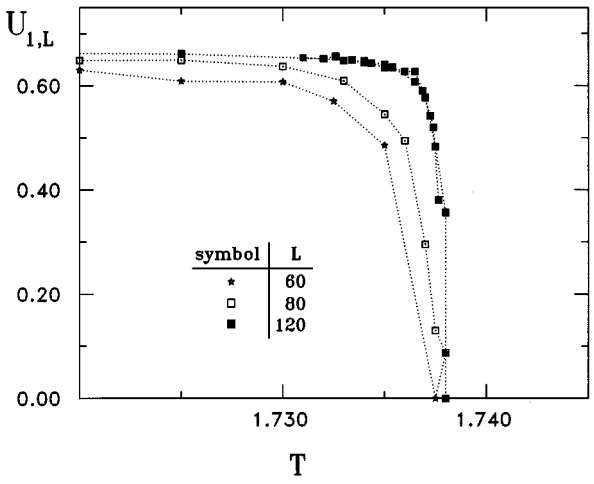

FIG. 13. Cumulants $U_{1,L}$ for the order parameter at the (111) surface plotted vs temperature, for different choices of L as indicated.

V. RESULTS FOR (111) SURFACES

The behavior in this case is quite different from that seen in the previous section. There is no surface order above T_{cb} (Fig. 10) and only finite-size short-range order can be seen in the data. As the transition temperature is approached from below, order-parameter profiles (see Fig. 11) reveal that a somewhat disordered layer appears at the surface and the interface between this layer and the bulk order moves into the bulk as the transition is approached. The disordering behavior is reflected in the disappearance of surface order as $T \to T_{cb}$ even though the bulk remains quite well ordered. We have analyzed ψ_1 for power-law behavior and find, from Fig. 12, that as the bulk transition temperature is approached, the data slowly enter an asymptotic regime where they are well described by

$$\psi_1 \propto (1 - T/T_{cb})^{\beta_1} = t^{0.64(2)}. \tag{41}$$

Three different lattice sizes were used in the simulation. However, even close at T_{cb} there are no obvious finite-size effects for ψ_1 parameter. In order to look more closely to possible finite-size effects, we studied the size dependence of $|\psi_1|$ at T_{cb} as shown in Fig. 12(b); assuming a finite-size scaling law $|\psi_1| \propto L^{-\beta_1/\nu_\parallel}$ [which is plausible in view of Eqs. (6) and (7)] we find $\nu_\parallel \approx 0.60 \pm 0.02$. Note, that the theoretical value is $\nu_\parallel = 1/2$ [see Eq. (19)], which assumes that the fluctuations in the surface plane are still governed by the fluctuations along the interface. The comparison with the data for a completely disordered film reveals that, at least for large systems, there remains only a trivial finite-size effect, which may have nothing to do with SID. One has to conclude that ψ_1 is not affected by $\nu_\parallel$ and that the scaling law assumed above does not apply here. Remember, that $\langle \psi_1^2 \rangle = (1/L^2) \Sigma_i \langle \psi_0 \psi_i \rangle \geq 1/L^2$ and that $\langle |\psi_1| \rangle$ is of the same order as $\langle \psi_1^2 \rangle^{1/2}$. Therefore finite-size scaling ideas are applicable only if $\beta_1/\nu_\parallel < 1$.

We also attempted to locate the transition from the cumulant crossings for different sizes (Fig. 13); however, we find no well-defined intersection point for any nonzero value of U_1. This result can already be expected from the missing finite-size effects above, and further, as will be shown below, also because the layer susceptibilities $\chi_{1,1}$ do not diverge as $T \to T_{cb}$.

In Fig. 14 we analyze the surface excess order parameter and surface excess energy. Both quantities are nicely compatible with the expected[7,9–12] logarithmic variation as T approaches T_{cb}. Similarly, the behavior of the surface excess specific heat is compatible with $C_s \propto t^{-1}$, as expected [see Eqs. (36) and (37)].

The critical behavior of the different surface related susceptibilities is analyzed in Fig. 15. Similar to the slow asymptotic behavior of ψ_1 and the excess quantities ψ_s and E_s, for $t < 0.003$ the surface susceptibility χ_1 and the surface excess susceptibility χ_s become at least compatible with the expected exponents, $\gamma_1 = 0.36$ as determined from β_1 and the scaling relation Eq. (17a), and $\gamma_s = 1$ (universal) as theoretically predicted[7,9–12] [see Eq. (16a)]. In our simulations agreement was obtained for estimates of these two susceptibilities from the appropriate fluctuation relations as well as from the variation with the conjugate field H [shown in Figs. 15(c) and 15(d)] according to their definition as derivatives in Eqs. (4b) and (4c). We have not presented as much data for the susceptibilities as we did for the order parameters,

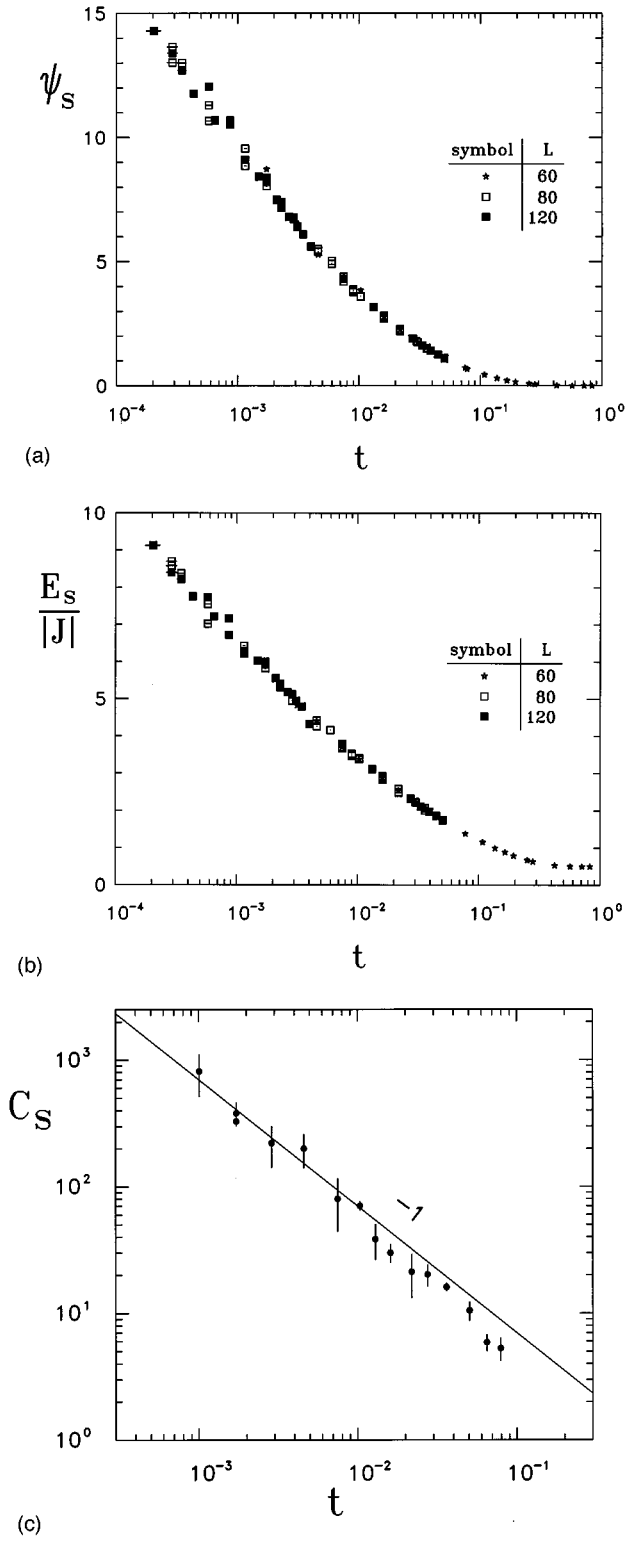

FIG. 14. (a) Semi-log plot of (111) surface excess order parameter vs $t=1-T/T_{cb}$. Different symbols show different lattice sizes L; (b) same as (a) but for the surface excess energy; (c) Log-log plot of the surface excess specific heat vs t. Straight line with slope -1 corresponding to $\alpha_s=1$ is included for comparison.

because the derivatives need longer MC runs and more CPU time. Our value $\beta_1\approx 0.64$ would imply also $\gamma_{11}\approx -0.28$, a result which is nicely compatible with the data which are shown in Fig. 15(e). In order to analyze the critical behavior of χ_{11}, we have subtracted the susceptibility contribution to χ_{11} in a disordered bulk, estimating this constant simply from a simulation of a disordered system at T_{cb} (which is equivalent to the case when the interface disappears towards infinite distance from the surfaces).

All results are in accordance with the scaling relations [Eqs. (17a)–(17d)] although one can see that the asymptotic region is approached rather slowly by the susceptibility data. One may also note that the verification of critical wetting theory for the standard Ising model has been notoriously difficult.[29–31]

In view of the exponents which we find, our model system belongs to the first scaling regime of Eq. (24a) for a rough interface. At this point, we recall that Lipowsky[7,9–12] has predicted (universal) mean-field exponents for SID for the case of smooth interfaces only, i.e., $\beta_1=1/2$, $\gamma_1=1/2$, $\gamma_{1,1}=0$, etc. That the interface is not smooth may be obvious from the layer profiles (see Fig. 12) which reveal finite and modest gradients at the positions of the interface. However, as opposed to the situation of an interface in the bulk (APB) for $T<T_{cb}$, the interface is bound to the surface and is not rough in the sense of the Kosterlitz-Thouless theory that it makes arbitrary excursions with increasing size of the system. Therefore, we examined the interfacial roughness in the limit $T\to T_{cb}$ where the interface becomes unbound from the surface. From the layer profiles we obtained a fit to Eq. (39) the interface position $\hat{n}$ and the interface width $\xi_\perp$. A typical example in case of a free (111) surface is shown in Fig. 16(a). The slight deviations near the surface (being unimportant for the present considerations) stem from the missing bonds at the free surface. At $T=T_{cb}$,[51] the procedure is carried out for a wide range of lateral dimensions L parallel to the surface, and the logarithmic divergence of ξ^2 is clearly seen [Fig. 16(d)]. Of course, this divergence is only possible in the limit $T\to T_{cb}$, where $\hat{n}$ also diverges, but for the temperatures considered the saturation of ξ at a finite value (due to the finiteness of $\hat{n}$) is not yet seen for the range of L displayed here.

Finally, our analysis of the interface profiles enables us to check the validity of the theoretical predictions[7] of the temperature dependence of the interface position (and thus of the surface layer thickness of the wetting phase, $l=\hat{n}-1/2$) and the width of the interface itself, as given in Eqs. (25) and (26). The results shown in Figs. 16(b) and 16(c) confirm both a logarithmic law for the position (which already followed from the behavior of the excess quantities ψ_s and E_s) as well as a root logarithmic law for the interfacial thickness. However, while Eqs. (25) and (26) can be fitted to the data in this case, there are some problems with the numbers that follow. One may note, that there is an additional constant term (which is related to the depinning temperature of the interface). While further the proportionality is even consistent with the value for $\omega=0.28$ [using our value of $\beta_1=0.64$ and Eq. (24a)], the bulk correlation length, $\xi_d=7.3(5)$ [in units of $(\sqrt{3}/4)a$], is obviously larger than the bulk correlation length as determined from independent simulations of the disordered bulk phase (see Fig. 4). As already discussed for the case of a free (100) surface, the problems may arise from the strong anisotropy of the correlations even in the disordered phase. And we again draw attention to the corrections that

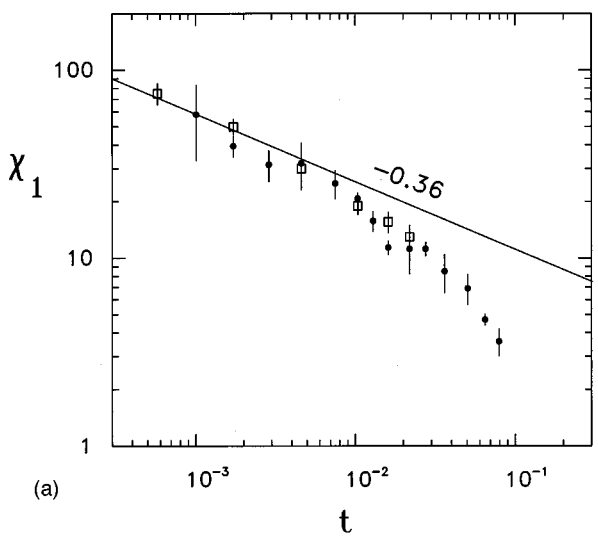

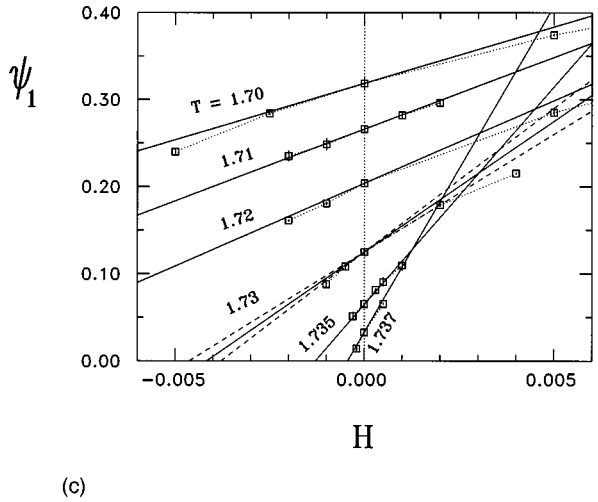

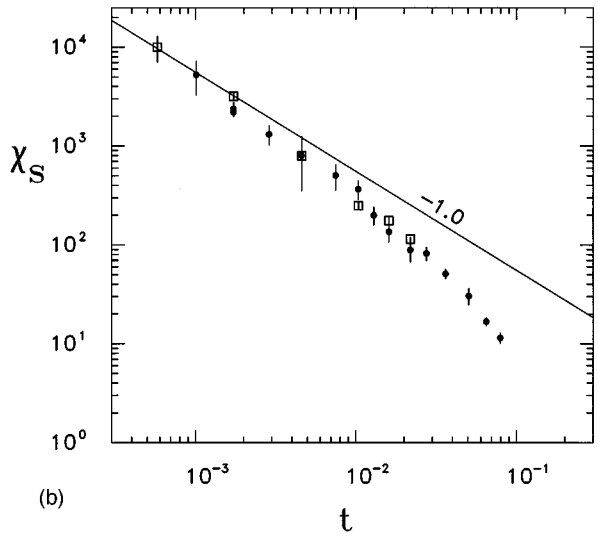

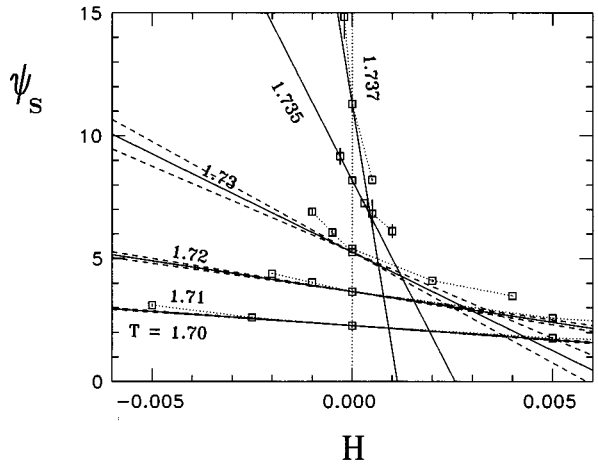

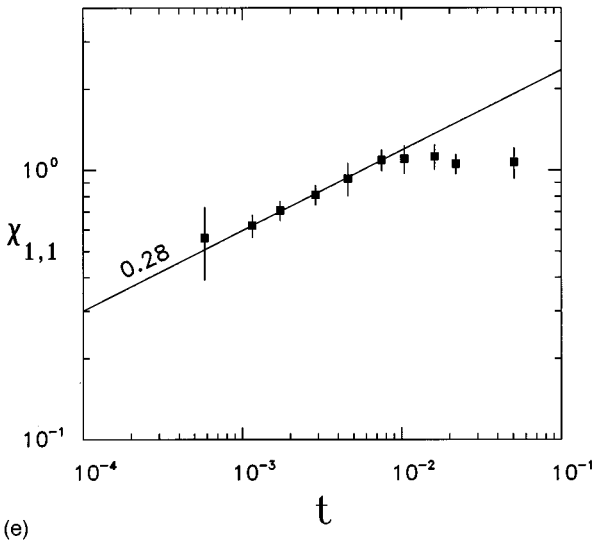

FIG. 15. Log-log plot of the (111) surface susceptibilities χ_1 (a) and χ_s (b) vs t. Filled dots are data calculated according to the fluctuation relations using Eqs. (33) and (34); open squares represent equivalent data obtained as the derivatives of $\psi_1(H)$ and $\psi_s(H)$ which are shown in (c) and (d), respectively; (e) shows the singular part of $\chi_{1,1}$ vs t using Eq. (32). Straight lines indicate the expected exponents (a) $\gamma_1 = 0.36$, (b) $\gamma_s = 1$, and (e) $\gamma_{1,1} = -0.28$, respectively. In parts (c) and (d) the broken straight lines indicate the error estimates for the fits, while the dotted curves through the data points are intended to guide the eye.

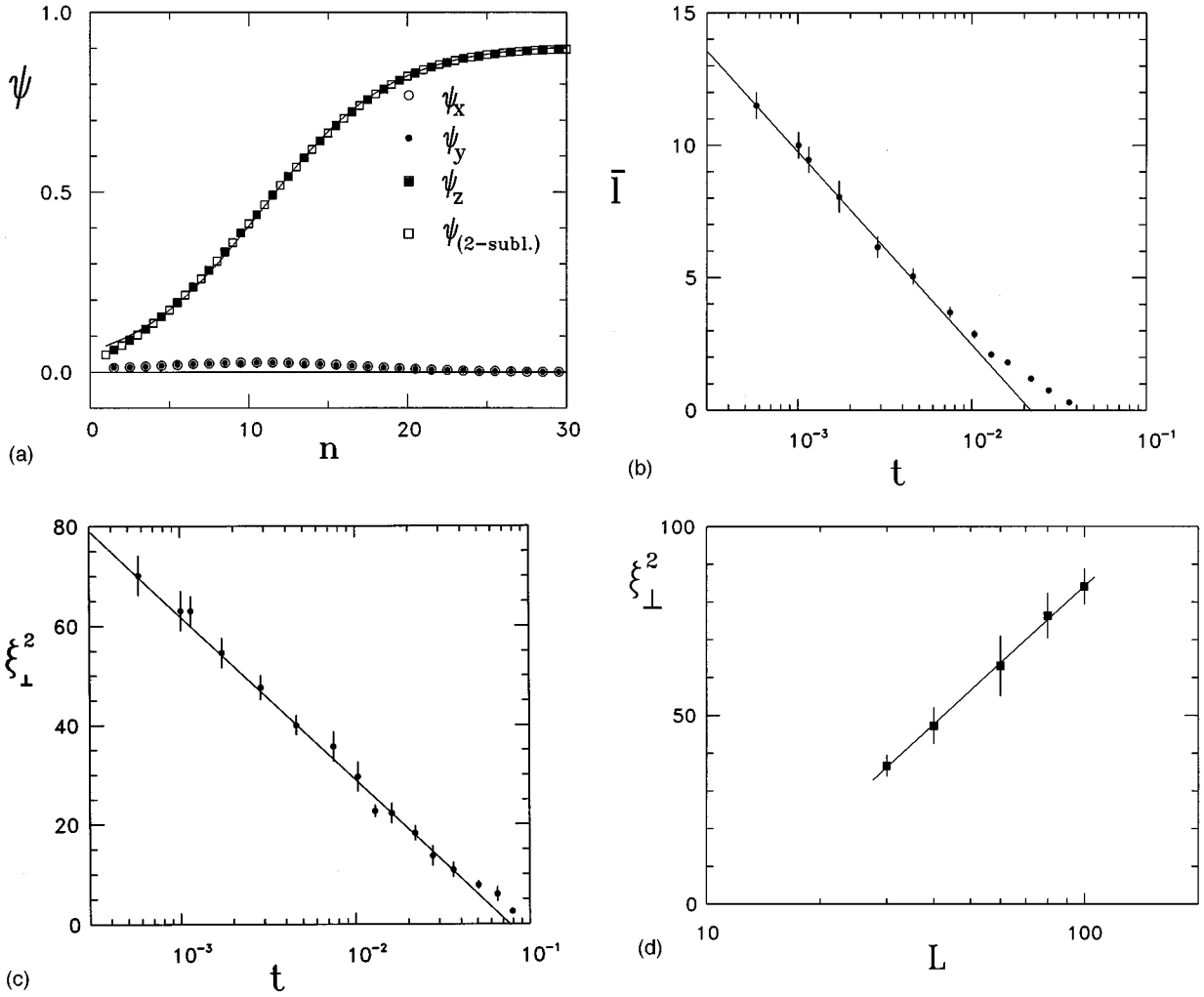

FIG. 16. (a) Determination of the interfacial width $\xi_\perp$ for the case of a (111) surface by fitting the observed profile (data points, and broken curve) to Eq. (39), for $T=1.734$. Here a system of size $120\times120\times160$ is used, and fit parameters are $\hat{n}=8.22$, $\xi_\perp=6.94$. (b) The thickness of the disordered surface layer $\bar{l}$ vs t, and (c) the squared thickness of the interface $\xi_\perp$ vs t exhibit asymptotically a logarithmic divergence. (d) Semi-log plot of the squared width vs the lateral linear dimension L at T_{cb} to demonstrate the logarithmic divergence expected for rough interfaces. Here $T=1.738$ is shown where for $L=200$, $\hat{n}$ was about 30 ± 6.

may result from the coupling of the interface position $\bar{l}$ to the length scale l_1 over which the surface modifies the tanh profile, Fig. 16(a), which were discussed by Boulter and Parry.[28]

VI. CONCLUSIONS

We have presented an extensive Monte Carlo study of surface phase transitions in a very simple model for AB binary alloys on a face-centered-cubic lattice. For the case of a (100) surface we have found a continuous surface transition at T_{cs} which is above the bulk transition temperature T_{cb} and surface-induced ordering as T_{cb} is approached from above. Qualitatively, the occurrence of this SIO is plausible due to the existence of ''frustrated'' interactions in the bulk ordered structure, while no frustrated interactions occur in the (100) surface. We find that the surface transition belongs to the universality class of the two-dimensional Ising model.

For (111) surfaces we find instead that the surface order parameter vanishes continuously right at the bulk transition temperature. In this case interactions are frustrated both in the bulk and in the surface plane. All of the various quantities which we studied confirm the essential predictions of the actual wetting theory that there is only a single independent critical exponent, further the values of the expected universal exponents, and also the scaling relations derived for SID. We find clear evidence that the exponent β_1 differs from its mean-field value. This fact implies that the fluctuation corrections proposed for critical wetting are indeed relevant here. Concerning the possible interfaces in the bulk, we expect that slightly below T_{cb} the APB's in (111) planes to be more rough than those in (100) planes, while the latter should occur more often because of their lower energies.

We hope that this work will stimulate corresponding experimental studies. While there are quite a number of experiments related to SID, in particular there is no experimental work showing SIO in alloys. We have no doubt that this may be a quite typical phenomenon and does not result merely from the special choice of the interaction model. SIO may be

TABLE I. Results for T_{cb} in units of $|J|/k_b$.

T_{cb}	Method	Reference
1.893	CVM-T (cluster variation method, tetrahedron approximation)	40
1.746(5)	High- and low-temperature series	41
1.71	MC (Monte-Carlo)	42
1.766(4)	MC	43
1.810	CVM-TO (tetrahedron-octahedron)	44
1.73	MC	45
1.745	"Mixed" CVM (TO and 13–14 point clusters)	46
1.736(1)	MC	47
1.738005(50)	MC	This work

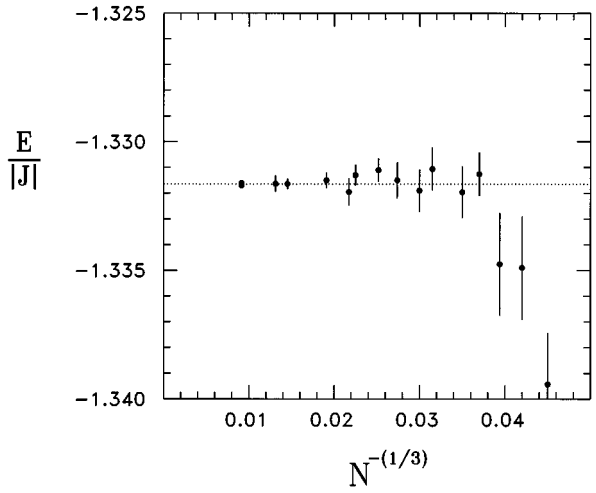

FIG. 17. Energy E versus $N^{-1/3}$ slightly above T_{cb}, at $T=1.7391$, for the disordered phase. Here, full periodic boundary conditions are used. Finite-size effects become negligible for data at large N.

expected, for instance, in particular in those alloys where long period ordered structures have been observed indicating the low energy of antiphase boundaries. SIO may occur whenever a free surface favors a particular ordering variant, in particular, if the ordered ground state has a lower than cubic symmetry. Therefore, at first sight one would not expect SIO in alloys like Cu_3Au. However, the presence of a surface always lowers the symmetry of the bulk state, and depending on the interaction model SIO may take place for any alternating order-parameter profile perpendicular to a free surface. As will be discussed in another publication, the presence of sufficiently strong (uniform) surface fields can also lead to SIO. In Appendix B we present arguments, however, that weak uniform surface fields (which are expected to occur in real alloys) would not change the phenomena qualitatively.

ACKNOWLEDGMENTS

This work was partially supported by the National Science Foundation (NSF) under Grants No. DMR-9100692 and DMR-9405018, by the Deutsche Forschungsgemeinschaft (DFG) under Grant No. SFB 262/D1, by the Alexander von Humboldt Stiftung, and by the collaborative NATO Grant No. CRG 921202. We are grateful to R. Lipowsky for helpful comments on the manuscript. One of the authors (W.S.) wishes to acknowledge W. Selke for discussions.

APPENDIX A: DETERMINATION OF THE BULK TRANSITION TEMPERATURE

A precise determination of the bulk transition temperature T_{cb} is needed in order for us to accurately extract the various critical exponents as given in this paper. Since the asymptotic region is reached very slowly ($t<0.01$) the uncertainty in t should be considerably less than 10^{-4} for there to be two decades in t for the determination of the exponents. Existing results in the literature are either incorrect or of insufficient accuracy for this purpose, as can be seen from Table I.

Various ways exist to determine T_{cb} for this first-order transition (see Refs. 52–55 for recent discussions). The MC data for the finite system having either a (111) or a (100) free surface could, in principle, be used for this purpose as well; however, in all cases one must eventually extrapolate to a system of infinite linear dimension perpendicular to the surfaces. Therefore, it is advantageous to consider the system without free surfaces and with fully periodic boundary conditions. A standard and well exploited method uses the integration with (inverse) temperature β of the specific heats.[54] Starting from states of known entropy, i.e., $T=\infty$ and $T=0$, one determines the free energy for the disordered and ordered branch. In order to obtain a reliable value for T_{cb}, as well as a reliable estimate for its range of confidence, one needs to carefully consider not only the apparent statistical errors but also all possible sources of systematic errors. We therefore carefully examined size effects, the quality of random numbers, and effects due to the manner in which the MC algorithm sweeps and selects sites in the crystal. Hence, (i) we studied the finite-size effects and different choices of distances between selected sites sligthly above T_{cb}, (ii) in the high-T limit we compared the simulated results to exact high-T series expansion, (iii) we used different integration schemes.

The simulations were performed using a single-site spin-flip algorithm. The size of the system finally used was 4×69^3, i.e., it consisted of four simple cubic sublattices each of equal linear dimensions $L=69$, containing in total more than 1.3 million Ising spins. For this size the correlation length always remained much smaller than L and finite-size effects did not introduce any significant systematic error [cf. Fig. 17, $E(N)$ at $T=1.7391$]. The number of MC steps per site ranged from 1000 far from the transition temperature to 5000 close to T_{cb} (this choice was determined by the energy fluctuations). Each update of the entire lattice was used in computing averages; however, for a proper estimate of the statistical error each MC run was analyzed in parts, chosen such that the averages taken for these did not show any correlations for subsequent data. We used 100 data points for the energies of the disordered high-T branch and 134 values for the low-T branch. The density of points was chosen approximately proportional to the curvature of the smooth function $E(T)$ [or $E(\beta)$], such that all contributions

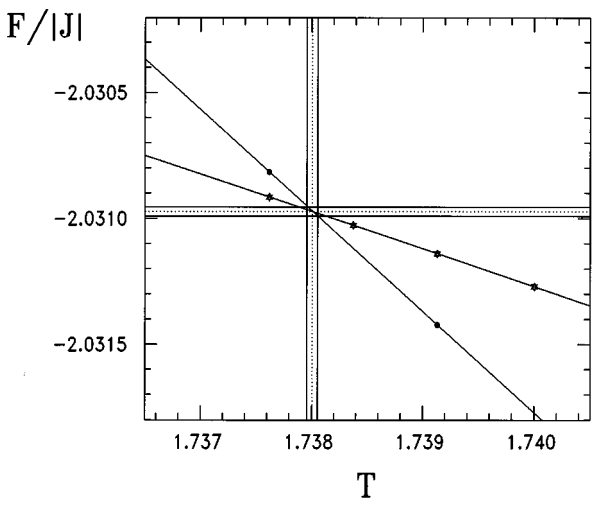

FIG. 18. Free energy versus temperature as calculated by thermodynamic integration for a large system (4×69^3 atoms) with fully periodic boundary conditions. The first-order bulk transition temperature T_{cb} is determined by the crossing of the branches for disordered and ordered phase.

to the integral have a similar statistical variance. The large number of data is a computational advantage, since by integration all data contribute to reduce the statistical error.

The high-T series for the nearest-neighbor pair-correlation function is

$$\langle s_i s_j\rangle_{i-j=1}=\sum w_n \tanh^n(\beta J), \tag{A1}$$

where the first leading coefficients are $w_1=-1$, $w_2=4$, $w_3=-28$ and $w_4=68$.

For the integration we used the simplest Newton-Cotes formulas, i.e., the trapezoidal rule and Simpson rule, as well as cubic spline approximations. The comparison of the different integration methods allows us to estimate any possible systematic errors introduced by the integration procedures. The integration based on cubic spline approximations is more precise than the Newton-Cotes rules; however, since the energy as a function of the (inverse) temperature is a rather smooth function, the trapezoidal and Simpson rules already yield quite similar results. (For comparison, the trapezoidal and Simpson rules yield $T_{cb}=1.738\ 16|J|/k_B$ and $T_{cb}=1.738\ 01|J|/k_B$, respectively). While the cubic splines have no specific requirements to the data basis, this allows us to estimate systematic errors resulting from different choices for the location and number of nodes. Figure 18 illustrates the behavior of the two branches of the free energy near the intersection point.

To summarize our results, we obtained the following:

$$T_{cb}=(1.738\ 005\pm0.000\ 05)|J|/k_B,$$

$$F_{cb}=(-2.030\ 97\pm0.000\ 02)|J|,$$

$$E_-=(-1.7729\pm0.0003)|J|,$$

$$E_+=(-1.3323\pm0.0002)|J|, S_-=(0.1485\pm0.0003)k_B,$$

$$S_+=(0.4020\pm0.0002)k_B. \tag{A2}$$

These error bars contain statistical as well as the estimated systematic uncertainties at a 95% confidence level (twice the standard deviations). Statistical errors are twice as large as the systematic ones.

APPENDIX B: DISCUSSION OF GROUND STATES AND THE EFFECT OF A UNIFORM SURFACE LAYER FIELD

As is well known, in an Ising-type description of a binary alloy AB three pairwise interactions are present, E_{AB}, E_{AA}, and E_{BB}, but for the description of bulk behavior only the combination $E_{AB}-(E_{AA}+E_{BB})/2$ matters (which translates into the exchange constant J of the equivalent Ising magnet), since the other relevant combination $E_{AA}-E_{BB}$ can be absorbed in the scale of the chemical potential difference between the species. At a surface, however, this is no longer true.[1] The effect of missing neighbors is to generate a term $H_1^{(1\times1)}\Sigma S_i$ in the Ising Hamiltonian, with $H_1^{(1\times1)}$ proportional to $E_{AA}-E_{BB}$ with the sum restricted to the spins in the surface plane. { Note, that we use the superscript "(1×1)" to distinguish this uniform field from the staggered field H_1 [Eq. (4a)], which is conjugated to the (2×2) superstructure in the surface layer.} In addition, the surrounding medium may act with different forces on A and B species in the surface layer, and hence this again results in a contribution of the above form, $H_1^{(1\times1)}\Sigma S_i$. Here we restrict ourselves for simplicity to short-range forces only, ignoring possible effects on more distant layers in this qualitative discussion.

Since in a real system the effect of a term $H_1^{(1\times1)}\Sigma S_i$ in the Hamiltonian is always present, it is important to make sure that it does not completely invalidate the description of the phenomena of SIO and SID in our model, where such a term was ignored so far. We first discuss the ground-state behavior at $T=0$, assuming our orientation of the ordered domains as shown in Fig. 1 (stacking of planes $ABAB$ along the z axis). Now simple bond counting yields the following results for the energies per spin:

$$E_{\rm bulk}=-2|J|, \tag{B1}$$

$$E_{(100)}=E_{(010)}=-2|J|, \tag{B2}$$

$$E_{(001)}=H_1^{(1\times1)}, \tag{B3}$$

$$E_{(111)}=-3|J|/2. \tag{B4}$$

Note that for (100), (010), and (111) surfaces the energies per spin in the surface planes do not depend on $H_1^{(1\times1)}$, because for the assumed stacking they all contain an equal number of A and B atoms. From the fact that $E_{(111)}$ is enhanced in comparison to $E_{\rm bulk}$, it is already plausible that surface-induced disordering should occur for (111) surfaces, since they are energetically less stable than the bulk. On the other hand, for (100) and (010) surfaces— which are equivalent by symmetry, of course—the energy of spins in the bulk and at the surface is the same. Thus, simple "bond counting" arguments cannot prove that surface-induced ordering should occur, entropic effects are crucial to stabilize the order in the surface plane at higher temperatures than in the bulk. Since

this is an entropic effect, it it not surprising that SIO exists in our model only at temperatures up to about 10% higher than T_{cb}.

For large enough fields the (001) surface is more stable than the (100) and (010) surfaces, namely for

$$H_1^{(1\times1)} > H_{1c}^{(1\times1)} = 2|J|. \tag{B5}$$

Alternating A, B planes parallel to the surfaces are more stable than the (2×2) structure. Thus, when one cuts an fcc crystal along an (100) plane such that one has a plate geometry where two surfaces have much larger area than all other surfaces, the degeneracy among the three types of domains (stacking of $ABAB\ldots$ planes along the x axis, y axis or z axis) is lifted by surface effects: if Eq. (B5) holds, the ordering of the crystal will be such that the planes of pure A and pure B are parallel to the surfaces, while for $H_1^{(1\times1)} < H_{1c}^{(1\times1)}$, the arrangement shown in Fig. 1(a) (and studied at finite temperatures for $H_1^{(1\times1)}=0$ in Sec. IV of this paper) will be the energetically preferred one.

Of course, at finite temperature a field $H_1^{(1\times1)}>0$ will have interesting effects on the SIO and SID behavior. E.g., in the case of the (2×2) structure in the (100) plane [Fig. 1(a)] the A-rich and B-rich sublattice of the surface plane are no longer equivalent (just as a magnetic field breaks the symmetry between the two sublattices of a simple antiferromagnet, enhancing the sublattice magnetization along the field direction and diminishing the sublattice magnetization with opposite orientation). However, we expect that the resulting surface enrichment effect will only lead to a shift of T_{cs}, and a short-range perturbation of the order parameter and energy profiles should result, while qualitatively the phenomena remain the same.

APPENDIX C: FLUCTUATION RELATIONS FOR THE SURFACE EXCESS SUSCEPTIBILITIES AND SPECIFIC HEATS

We consider the free-energy density of a thin film of thickness D and a lateral size of $L\times L$ (in absence of any surface fields $H_1=0$ for simplicity):

$$\frac{F}{L^2D} = f_b(T,H) + \frac{2}{D} f_s(T,H) = f_{\rm film}(T,H). \tag{C1}$$

An analogous decomposition holds trivially for all derivatives, in particular for the magnetization per spin in the film:

$$m_{\rm film} = -\frac{1}{L^2D}\left(\frac{\partial F}{\partial H}\right)_T = m_b + \frac{2}{D} m_s(T,H) \quad as \quad D\to\infty, \tag{C2}$$

with

$$m_b = -\left(\frac{\partial f_b}{\partial H}\right)_T,$$

$$m_s = -\left(\frac{\partial f_s}{\partial H}\right)_T, \tag{C3}$$

and the susceptibility per spin

$$\chi_{\rm film} = \left(\frac{\partial m_{\rm film}}{\partial H}\right)_T = -\frac{1}{L^2D}\left(\frac{\partial^2 F}{\partial H^2}\right)_T = \chi_b + \frac{2}{D}\chi_s(T,H), \tag{C4}$$

with

$$\chi_b = -\left(\frac{\partial m_b}{\partial H}\right)_T \left(\frac{\partial^2 f_b}{\partial H^2}\right)_T,$$

$$\chi_s = -\left(\frac{\partial m_s}{\partial H}\right)_T \left(\frac{\partial^2 f_s}{\partial H^2}\right)_T. \tag{C5}$$

Since $F_{\rm film}$, $m_{\rm film}$, $\chi_{\rm film}$ are densities of additive variables [$F(T,H)$ and its derivatives are extensive thermodynamic variables], we can write them as sums over layer quantities:

$$f_{\rm film} = \frac{F}{L^2D} = \frac{1}{D}\sum_{n=1}^{D} f_n(T,H), \tag{C6}$$

where $f_n(T,H)$ denotes the free energy per spin in the nth layer. This also holds for the derivatives

$$m_{\rm film} = \frac{1}{D}\sum_{n=1}^{D} m_n(T,H),$$

$$\chi_{\rm film} = \frac{1}{D}\sum_{n=1}^{D} \chi_n(T,H), \tag{C7}$$

where

$$m_n = -\left(\frac{\partial f_n}{\partial H}\right)_T,$$

$$\chi_n = \left(\frac{\partial m_n}{\partial H}\right)_T = -\left(\frac{\partial^2 f_n}{\partial H^2}\right)_T. \tag{C8}$$

Now we know that in the considered limit ($D\to\infty$) the profiles f_n, m_n, χ_n ultimately reach their bulk values in the center of the film, and thus it makes sense to rewrite $f_n(T,H)$, $m_n(T,H)$, $\chi_n(T,H)$ as follows:

$$f_n = f_n - f_{D/2} + f_{D/2}, \ \text{etc.} \tag{C9}$$

and hence (assuming an even number of layers, but this is not really essential)

$$f_{\rm film} = \frac{2}{D}\sum_{n=1}^{D/2} f_n(T,H) \tag{C10}$$

$$= f_b(T,H) + \frac{2}{D}\sum_{n=1}^{\infty} \{f_n(T,H) - f_b(T,H)\}. \tag{C11}$$

Putting ∞ instead of $D/2$ in the last step is allowed, because $f_n(T,H)-f_b=0$ near $n=D/2$, so we add only zeros. Comparing Eqs. (C1) and (C10) we see that

$$f_s(T,H) = \sum_{n=1}^{\infty} \{f_n(T,H) - f_b(T,H)\}. \tag{C12}$$

Obviously this reasoning goes through for any derivatives, e.g.,

$$m_{\text{film}}=m_b(T,H)+\frac{2}{D}\sum_{n=1}^{\infty}\{m_n(T,H)-m_b(T,H)\}, \tag{C13}$$

$$m_s(T,H)=\sum_{n=1}^{\infty}\{m_n(T,H)-m_b(T,H)\} \tag{C14}$$

and

$$\chi_{\text{film}}=\chi_b(T,H)+\frac{2}{D}\sum_{n=1}^{\infty}\{\chi_n(T,H)-\chi_b(T,H)\}, \tag{C15}$$

$$\chi_s(T,H)=\sum_{n=1}^{\infty}\{\chi_n(T,H)-\chi_b(T,H)\}. \tag{C16}$$

Of course, this is also compatible with the fluctuation relations, since we can simply start from the susceptibility fluctuation relation for the total film

$$k_BT\chi_{\text{film}}=\frac{1}{L^2D}\left\{\left\langle\left(\sum_\nu s_\nu\right)^2\right\rangle-\left\langle\sum_\nu s_\nu\right\rangle^2\right\}$$

$$=\frac{1}{L^2D}\sum_{\mu\nu}\{\langle s_\mu s_\nu\rangle-\langle s_\mu\rangle\langle s_\nu\rangle\}. \tag{C17}$$

Due to the translational invariance in the directions parallel to the free surfaces we can decompose the summation over μ in a sum over the μ' spins in the layer, and the sum n over layers:

$$\chi_{\text{film}}=\frac{1}{D}\sum_n \chi_n, \quad \text{with}$$

$$k_bT\chi_n=\sum_{0,\nu}(\langle s_0 s_\nu\rangle-\langle s_0\rangle\langle s_\nu\rangle). \tag{C18}$$

where ν denotes any site in the system and 0 an element of the nth layer. The formula for χ_n can also be written as

$$k_bT\chi_n=L^2D(\langle\Psi_n\Psi\rangle-\langle\Psi_n\rangle\langle\Psi\rangle) \tag{C19}$$

(derivation exactly as shown before for $n=1$). The order parameter in the nth layer has to be correlated with the order in the whole film. Of course, the exactly analogous formulas hold for derivatives with respect to temperature, and hence since the energy per spin of the whole film

$$e_{\text{film}}=e_b+\frac{2}{D}e_s=\frac{1}{D}\sum_{n=1}^{D}e_n, \tag{C20}$$

we have for the specific heats per spin

$$c_{\text{film}}=c_b+\frac{2}{D}c_s=\frac{1}{D}\sum_{n=1}^{D}c_n \tag{C21a}$$

and for the surface excess specific heat

$$c_s=\sum_{n=1}^{\infty}(c_n-c_b). \tag{C21b}$$

Since

$$c=\frac{\partial e}{\partial T}=\frac{\partial e}{\partial\beta}\frac{\partial\beta}{\partial T}=-\frac{1}{T^2}\frac{\partial e}{\partial\beta}$$

($k_B=1$), from $e=\langle\mathscr{H}\rangle$ or $L^2De_n=\langle\mathscr{H}_n\rangle=\mathrm{Tr}\mathscr{H}_n e^{-\beta\mathscr{H}}/\mathrm{Tr}e^{-\beta\mathscr{H}}$ we conclude

$$T^2c_n=(L^2D)^{-1}(\langle\mathscr{H}_n\mathscr{H}\rangle-\langle\mathscr{H}_n\rangle\langle\mathscr{H}\rangle),$$

where $\mathscr{H}$ denotes the total Hamiltonian, while both $\mathscr{H}_n$ and $\mathscr{H}$ are unnormalized Hamiltonians. The correct expression for c_s hence is

$$T^2c_s=\frac{1}{L^2D}\sum_n\{\langle\mathscr{H}_n\mathscr{H}\rangle-\langle\mathscr{H}_n\rangle\langle\mathscr{H}\rangle-\langle\mathscr{H}_{D/2}\mathscr{H}\rangle$$

$$-\langle\mathscr{H}_{D/2}\rangle\langle\mathscr{H}\rangle\}. \tag{C22}$$

Note that c_b has to be calculated as

$$T^2c_b=\frac{1}{L^2D}\{\langle\mathscr{H}_n\mathscr{H}\rangle-\langle\mathscr{H}_n\rangle\langle\mathscr{H}\rangle\}_{n=D/2}, \tag{C23}$$

and *not* as

$$T^2c_{n,n}=\frac{1}{L^2D}\{\langle\mathscr{H}_n\mathscr{H}_n\rangle-\langle\mathscr{H}_n\rangle\langle\mathscr{H}_n\rangle\}_{n=D/2}, \tag{C24}$$

which is the analog of a layer susceptibility in the bulk. For calculating the specific heat in the bulk, one must correlate the energy in the bulk layer $n=D/2$ with the total energy $\mathscr{H}$ of the film, not just with the energy in that layers (otherwise transverse energy-energy correlations would be missing). Apparently, neither the surface excess specific heat c_s nor the surface excess susceptibility χ_s would be correctly obtained by considering [instead of Eqs. (C15) and (C21b)] the fluctuation relations of the surface excess energy or the surface excess magnetization, respectively.

[1] For reviews of surface critical phenomena, see K. Binder, in *Phase Transitions and Critical Phenomena*, edited by C. Domb and J.L. Lebowitz (Academic, New York, 1983), Vol. 8, Chap. 1.

[2] H.W. Diehl, in *Phase Transitions and Critical Phenomena*, edited by C. Domb and J.L. Lebowitz (Academic, New York, 1986), Vol. 10, p. 75.

[3] For reviews of wetting phenomena, see S. Dietrich, in *Phase Transitions and Critical Phenomena*, edited by C. Domb and J.L. Lebowitz (Academic, New York, 1988), Vol. 12, Chap. 1, and Ref. 2.

[4] D.E. Sullivan and M.M. Telo da Gama, in *Fluid Interfacial Phenomena*, edited by C.A. Croxton (Wiley, New York, 1986), p. 45.

[5] P.G. de Gennes, Rev. Mod. Phys. **57**, 825 (1985).

[6] M.E. Fisher, J. Stat. Phys. **34**, 667 (1984); J. Chem. Soc. Faraday Trans. **282**, 1569 (1986).

[7] R. Lipowsky, J. Appl. Phys. **55**, 2485 (1984); Ferroelectrics **73**, 69 (1987).
[8] H. Dosch, in *Critical Phenomena at Surfaces and Interfaces*, edited by G. Höhler, Springer Tracts in Modern Physics, Vol. 126 (Springer, Berlin, 1992).
[9] R. Lipowsky, Phys. Rev. Lett. **49**, 1575 (1982).
[10] R. Lipowsky, Z. Phys. B **51**, 165 (1983).
[11] R. Lipowsky and W. Speth, Phys. Rev. B **28**, 3983 (1983).
[12] R. Lipowsky, Z. Phys. B **55**, 335 (1984).
[13] V.S. Sundaram, B. Farrell, R.S. Alben, and W.D. Robertson, Phys. Rev. Lett. **31**, 1136 (1973).
[14] V.S. Sundaram, R.S. Alben, and W.D. Robertson, Surf. Sci. **46**, 653 (1974).
[15] E.G. McRae and R.A. Malic, Surf. Sci. **148**, 551 (1984).
[16] S.F. Alvarado, M. Campagna, A. Fattah, and W. Uelhoff, Z. Phys. B **66**, 103 (1987).
[17] H. Dosch, L. Mailänder, A. Lied, J. Peisl, F. Grey, R.L. Johnson, and S. Krumnacher, Phys. Rev. Lett. **60**, 2382 (1988); H. Dosch, L. Mailänder, H. Reichert, J. Peisl, and R.L. Johnson, Phys. Rev. B **43**, 13 172 (1991).
[18] B. Pluis, A.W. Denier van der Gon, J.F. van der Veen, and A.J. Riemersma, Surf. Sci. **239**, 265 (1990); B. Pluis, D. Frenkel, and J.F. van der Veen, *ibid.* **239**, 282 (1990).
[19] K.C. Prince, U. Breuer, and H.P. Bonzel, Phys. Rev. Lett. **60**, 1146 (1988).
[20] Ch. Ricolleau, A. Loiseau, F. Ducastelle, and R. Caudron, Phys. Rev. Lett. **68**, 3591 (1992).
[21] W. Schweika, K. Binder, and D.P. Landau, Phys. Rev. Lett. **65**, 3321 (1990).
[22] R. Lipowsky, D.M. Kroll, and R.K.P. Zia, Phys. Rev. B **27**, 4499 (1983); see also D. M. Kroll and R. Lipowsky, *ibid.* **28**, 6435 (1983).
[23] E. Brezin, B.I. Halperin, and S. Leibler, Phys. Rev. Lett. **50**, 1387 (1983).
[24] D.S. Fisher and D.A. Huse, Phys. Rev. B **32**, 247 (1985).
[25] R. Lipowsky and M.E. Fisher, Phys. Rev. B **36**, 2126 (1987).
[26] E. Brezin and T. Halpin-Healey, Phys. Rev. Lett. **58**, 1220 (1987); J. Phys. (Paris) **48**, 757 (1987).
[27] M.E. Fisher and A.J. Jin, Phys. Rev. Lett. **69**, 792 (1992); A.J. Jin and M.E. Fisher, Phys. Rev. B **47**, 7365 (1993); M.E. Fisher, A.J. Jin, and A.D. Parry, Ber. Bunsenges. Phys. Chem. **98**, 357 (1994).
[28] C.J. Boulter and A.O. Parry, Phys. Rev. Lett. **74**, 3403 (1995).
[29] K. Binder, D.P. Landau, and D.M. Kroll, Phys. Rev. Lett. **56**, 2276 (1986).
[30] K. Binder and D.P. Landau, Phys. Rev. B **37**, 1745 (1988); J. Appl. Phys. **57**, 3306 (1985).
[31] K. Binder, D.P. Landau, and. S. Wansleben, Phys. Rev. B **40**, 6971 (1989).
[32] K. Binder and D.P. Landau, Phys. Rev. B **46**, 4844 (1992).
[33] R. Lipowsky, Dissertation, University of München, 1982.
[34] K. Binder and D.P. Landau, Phys. Rev. Lett. **52**, 318 (1984); D.P. Landau and K. Binder, Phys. Rev. B **41**, 4786 (1990).
[35] K. Binder and D.W. Heermann, *The Monte Carlo Method in Statistical Physics. An Introduction* (Springer, Berlin, 1988).
[36] *Finite Size Scaling and the Numerical Simulation of Statistical Systems*, edited by V. Privman (World Scientific, Singapore, 1990).
[37] K. Binder, in *Computational Methods in Field Theory*, edited by C.B. Lang and A. Gausterer (Springer, Berlin, 1992), p. 59.
[38] T.W. Burkhardt and B. Derrida, Phys. Rev. B **32**, 7273 (1985); A.D. Bruce, J. Phys. A **18**, L873 (1985); D.P. Landau and D. Stauffer, J. Phys. (Paris) **50**, 509 (1989).
[39] J.W. Cahn and J.C. Hilliard, J. Chem. Phys. **28**, 258 (1958).
[40] R. Kikuchi and H. Sato, Acta Metall. **22**, 1099 (1974).
[41] D. F. Styer, Phys. Rev. B **17**, 2926 (1978).
[42] K. Binder, Phys. Rev. Lett. **45**, 811 (1980).
[43] M.K. Phani, J.L. Lebowitz, and M.K. Kalos, Phys. Rev. B **21**, 4027 (1980).
[44] A. Finel and F. Ducastelle, Europhys. Lett. **1**, 135 (1986).
[45] H.T. Diep, A. Ghazali, B. Berge, and P. Lallemand, Europhys. Lett. **2**, 603 (1986).
[46] A. Finel, in *Alloy Phase Stability*, NATO ASI Series E, edited by G.M. Stocks and A. Gonis (Kluwer, Dordrecht, 1989), p. 278.
[47] T.L. Polgreen, Phys. Rev. B **29**, 1468 (1984).
[48] D.P. Landau and K. Binder, Phys. Rev. B **41**, 4786 (1990).
[49] T.W. Burkhardt and H.W. Diehl, Phys. Rev. B **50**, 3894 (1994).
[50] A. Finel, in *Statics and Dynamics of Alloy Phase Transformations*, Vol. 319 of NATO ASI Series B: Physics, edited by P.E.A. Turchi and A. Gonis (Plenum, New York, 1994), p. 495.
[51] Long MC runs are required. Note that the accurate temperature in the simulation is also determined from the distribution of the selected random numbers.
[52] K. Binder, K. Vollmayr, H.-P. Deutsch, J.D. Reger, M. Scheucher, and D.P. Landau, in *Dynamics of First Order Phase Transitions*, edited by H.J. Herrmann, W. Janke, and F. Karrch (World Scientific, Singapore, 1992), p. 253.
[53] W. Janke, in *Computer Simulation Studies in Condensed Matter Physics VII*, edited by D.P. Landau, K.K. Mon, and H.-B. Schüttler (Springer, Berlin, 1994), p. 29.
[54] *Monte Carlo Methods in Statistical Physics*, edited by K. Binder (Springer, Berlin, 1979).
[55] A. Hüller, Z. Phys. B **93**, 401 (1994).